

Developmental Neurotoxicity of the Harmful Algal Bloom Toxin Domoic Acid: Cellular and Molecular Mechanisms Underlying Altered Behavior in the Zebrafish Model

Jennifer M. Panlilio,^{1,2,3*} Neelakanteswar Aluru,^{1,3} and Mark E. Hahn^{1,3}

¹Biology Department, Woods Hole Oceanographic Institution (WHOI), Woods Hole, Massachusetts, USA

²Massachusetts Institute of Technology (MIT)–WHOI Joint Graduate Program in Oceanography and Oceanographic Engineering, Department of Earth, Atmospheric and Planetary Sciences, MIT, Cambridge, Massachusetts, USA

³Woods Hole Center for Oceans and Human Health, WHOI, Woods Hole, Massachusetts, USA

BACKGROUND: Harmful algal blooms (HABs) produce potent neurotoxins that threaten human health, but current regulations may not be protective of sensitive populations. Early life exposure to low levels of the HAB toxin domoic acid (DomA) produces long-lasting behavioral deficits in rodent and primate models; however, the mechanisms involved are unknown. The zebrafish is a powerful *in vivo* vertebrate model system for exploring cellular processes during development and thus may help to elucidate mechanisms of DomA developmental neurotoxicity.

OBJECTIVES: We used the zebrafish model to investigate how low doses of DomA affect the developing nervous system, including windows of susceptibility to DomA exposure, structural and molecular changes in the nervous system, and the link to behavioral alterations.

METHODS: To identify potential windows of susceptibility, DomA (0.09–0.18 ng) was delivered to zebrafish through caudal vein microinjection during distinct periods in early neurodevelopment. Following exposure, structural and molecular targets were identified using live imaging of transgenic fish and RNA sequencing. To assess the functional consequences of exposures, we quantified startle behavior in response to acoustic/vibrational stimuli.

RESULTS: Larvae exposed to DomA at 2 d postfertilization (dpf), but not at 1 or 4 dpf, showed consistent deficits in startle behavior at 7 dpf, including lower responsiveness and altered kinematics. Similarly, myelination in the spinal cord was disorganized after exposure at 2 dpf but not 1 or 4 dpf. Time-lapse imaging revealed disruption of the initial stages of myelination. DomA exposure at 2 dpf down-regulated genes required for maintaining myelin structure and the axonal cytoskeleton.

DISCUSSION: These results in zebrafish reveal a developmental window of susceptibility to DomA-induced behavioral deficits and identify altered gene expression and disrupted myelin structure as possible mechanisms. The results establish a zebrafish model for investigating the mechanisms of developmental DomA toxicity, including effects with potential relevance to exposed sensitive human populations. <https://doi.org/10.1289/EHP6652>

Introduction

Domoic acid (DomA) is a potent neurotoxin that is produced by diatoms in the genus *Pseudo-nitzschia*. DomA exerts its toxicity by binding to and activating ionotropic glutamate receptors, particularly the α -amino-3-hydroxy-5-methyl-4-isoxazolepropionic acid (AMPA) and kainate (KA) subtypes (Hampson et al. 1992). Human exposure to DomA occurs primarily through the consumption of contaminated seafood. Acute exposure to high levels of DomA can lead to a syndrome called amnesic shellfish poisoning, with symptoms ranging from mild gastrointestinal issues to memory loss, seizures, coma, and death (Jeffery et al. 2004; Lefebvre and Robertson 2010; Perl et al. 1990b). To protect adults from these acute effects, regulatory limits of 20 μg DomA/g of shellfish tissue have been established and are recognized internationally (Mariën 1996; Pulido 2008; Wekell et al. 2004). However, seafood with measurable levels of DomA below these regulatory limits is still widely harvested and consumed. Epidemiological research suggests that chronic exposure to DomA at or below these

regulatory limits has consequences for learning and memory in adults (Grattan et al. 2018, 2016). Furthermore, these regulations may not be sufficiently protective for exposures that occur during embryonic and early postnatal development when animals are known to be more sensitive to DomA (Doucette et al. 2004; Tryphonas et al. 1990; Xi et al. 1997).

Research in animal models has demonstrated that developing animals can be exposed to DomA through both placental transfer and lactation. In rats, DomA readily crossed the placenta, making its way into the fetal brain and accumulating in fetal fluids (Maucher and Ramsdell 2007). In sea lions (Brodie et al. 2006; Lefebvre et al. 2018; Scholin et al. 2000) and cynomolgus monkeys (Shum et al. 2020), amniotic fluid was shown to serve as a reservoir for DomA, suggesting that fetuses could experience prolonged exposure to DomA following a single maternal exposure. DomA may also be transferred to breast milk. DomA was measured in the milk of sea lions consuming DomA-contaminated prey (Rust et al. 2014). In lactating rats injected with DomA, the toxin was detectable in both the maternal plasma and the milk, and persisted in the milk much longer than it did in the plasma (Maucher and Ramsdell 2005).

Lasting behavioral deficits can occur following either prenatal or postnatal exposure to DomA. These behavioral effects occur even at doses that do not lead to overt signs of toxicity either in mothers (in the case of prenatal exposures) or in the pups themselves (for postnatal exposures). Rodents exposed prenatally to DomA exhibited aberrant exploratory behaviors (Levin et al. 2005; Tanemura et al. 2009) subtle motor coordination deficits (Shiotani et al. 2017), and in some cases deficits in contextual learning (Shiotani et al. 2017; Tanemura et al. 2009). Rodents exposed postnatally displayed seizures when exposed to novel environments (Doucette et al. 2004; Perry et al. 2009) and also had aberrant drug-seeking behaviors as assessed by nicotine place preference tests (Burt et al. 2008a, 2008b).

Address correspondence to Jennifer M. Panlilio, MS #32, Woods Hole Oceanographic Institution, Woods Hole, MA 02543 USA. Email: jennifer.panlilio@nih.gov

Supplemental Material is available online (<https://doi.org/10.1289/EHP6652>).

*Current address: Jennifer M. Panlilio, Division of Developmental Biology, Eunice Kennedy Shriver National Institute of Child Health and Human Development, Bethesda, MD 20892 USA.

The authors declare they have no actual or potential competing financial interests.

Received 10 December 2019; Revised 18 September 2020; Accepted 28 September 2020; Published 4 November 2020.

Note to readers with disabilities: *EHP* strives to ensure that all journal content is accessible to all readers. However, some figures and Supplemental Material published in *EHP* articles may not conform to 508 standards due to the complexity of the information being presented. If you need assistance accessing journal content, please contact ehponline@niehs.nih.gov. Our staff will work with you to assess and meet your accessibility needs within 3 working days.

Although developmental exposure to DomA in rodents can lead to lasting behavioral deficits (Levin et al. 2006; Shiotani et al. 2017; Tanemura et al. 2009), the cellular and molecular mechanisms underlying these deficits are poorly understood. To elucidate these mechanisms, we used zebrafish as a model. Zebrafish have brain structures and sensory-motor pathways that are homologous to those of humans (Panula et al. 2010; Tropepe and Sive 2003). Furthermore, the transparency of zebrafish embryos and the availability of transgenic lines allow us to directly observe critical cellular processes and structural targets during early development *in vivo* (Fetcho and Higashijima 2004; Guo 2004; Higashijima et al. 2003; Sumbre and de Polavieja 2014). Moreover, larval zebrafish have simple behaviors that are driven by well-characterized neural circuits and comprised of known cell types, allowing us to link behavior to the underlying structural and cellular targets (Arrenberg and Driever 2013; Orger and de Polavieja 2017).

The goal of this study was to identify the behavioral, structural, and transcriptional changes from low-dose exposures to DomA during critical periods in early development. Using intravenous microinjection, we were able to deliver single doses at specific developmental times that spanned late embryonic [1 d postfertilization (dpf)] to larval stages (4 dpf). The dosages used were similar to those causing behavioral effects in developing rodents (Adams et al. 2008; Bernard et al. 2007; Doucette et al. 2004; Gill et al. 2010; Marriott et al. 2012; Perry et al. 2009; Tasker et al. 2005), and well below those associated with acute toxicity in adult humans (Perl et al. 1990a, 1990b).

We investigated whether exposure to DomA during a specific window in early development leads to disrupted myelination in the spinal cord and altered gene expression, and their association with behavioral deficits.

Materials and Methods

Fish Husbandry and Lines Used

These studies were approved by the Woods Hole Oceanographic Institution Animal Care and Use Committee (Assurance D16-00381 from the National Institutes of Health Office of Laboratory Animal Welfare). Fish were maintained in recirculating tank systems that were specifically designed for zebrafish culture (Aquatic Habitats Inc.). Temperature, lighting, and water quality were monitored daily and maintained according to recommendations from the Zebrafish International Resource Center. Fish were fed twice daily, once with live brine shrimp and once with the pellet feed Gemma Micro 300 (Skretting Inc.). The afternoon before breeding, males and females were separated with a divider. The morning of the breeding, dividers were removed, and embryo collectors—containers with mesh on the top that let embryos filter to a catch basin—were placed in tanks with multiple breeding pairs for batch breeding unless otherwise noted. Embryos were maintained at 28–28.5°C with a 14 h:10 h light–dark cycle during the experimental period. In experiments where daily morphological attributes were scored, fish were kept individually in 48-well plates; otherwise they were group housed in 6-well plates with 0.3× Danieau’s medium that was refreshed daily.

Larvae were not fed during the duration of the study (up to 7 dpf). Behavioral experiments are routinely done on unfed larvae up to 7 dpf (Schneider et al. 2012). Furthermore, lack of feeding through 8 d of larval life has not been shown to affect subsequent growth or survival of zebrafish through several weeks of life, suggesting that the lack of feeding through 7 d would not be a major source of stress for the fish (Hernandez et al. 2018).

The transgenic line *Tg(mbp:EGFP-CAAX)* in the AB background was used for acute neurotoxicity, behavioral assays,

RNA-seq, and myelin labeling experiments. This line was originally generated by the David Lyon’s lab (Almeida et al. 2011) and was generously provided by Sarah Kucenas’ lab. The double transgenic, [*Tg(nkx2.2a:mEGFP)* × *Tg(sox10:RFP)*] outcrossed to the AB background was used for time-lapse microscopy experiments. This line was a generous gift from Bruce Appel’s lab (Kirby et al. 2006; Kucenas et al. 2008).

DomA Exposure Paradigm

DomA (5 mg; see the section “Reagents” in the Supplemental Material) was dissolved directly in the vial with diluted embryo medium (0.2× Danieau’s) to obtain a 20 mM solution. This was immediately used to generate stock concentrations of 0.675 µg/mL and 1.4 µg/µL. Aliquots (10 µL each) were stored at –20°C. Experiments were completed within 19 months of generating the stock. Working solutions were prepared fresh prior to microinjection by diluting the stock to obtain the appropriate doses. Microinjection needles (see the section “Equipment” in the Supplemental Material) were created from glass capillary tubes and microinjections were performed to deliver 0.2 nL per embryo.

To determine the window of susceptibility for exposure at lower doses, DomA (0.09, 0.13, 0.14, 0.18 ng nominal dose) was intravenously microinjected into the common posterior cardinal vein at different developmental stages ranging from 1–4 dpf (Figure 1A) (Cianciolo Cosentino et al. 2010). Controls from the same breeding cohort were injected with the saline vehicle (0.2× Danieau’s). To perform intravenous microinjections, fish were manually dechlorinated using forceps then anesthetized with tricaine methanesulfonate (MS222; 0.10%) and placed laterally on dishes coated with 1.5% agarose. An injection was deemed

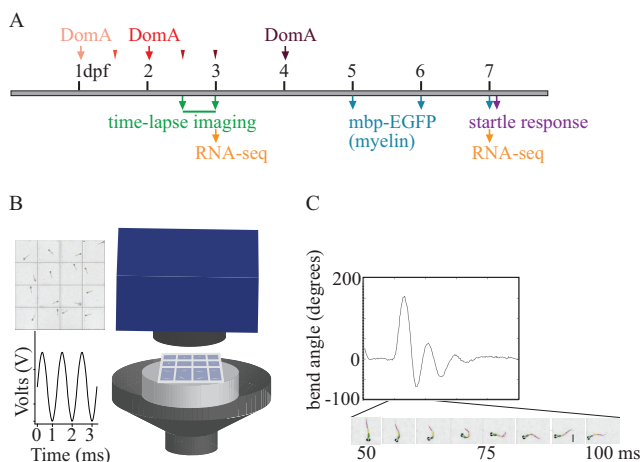


Figure 1. Experimental setup. (A) Exposure paradigm and end points assessed during zebrafish development. Domoic acid (DomA) was intravenously microinjected at one developmental time. Arrows indicate the three developmental time points that were used across all experiments [1, 2, and 4 d postfertilization (dpf)]. Thinner arrowheads represent other developmental time points at which DomA was injected in selected experiments (1.5, 2.5, and 3 dpf). For each injection category, the associated ranges of injection times in hours postfertilization (hpf) were: 1 dpf (28–32.5 hpf), 1.5 dpf (35.5–39 hpf), 2 dpf (47–53 hpf), 2.5 dpf (60–64 hpf), 3 dpf (71–77 hpf), and 4 dpf (99–105.5 hpf). Mortality, morphological defects, the presence or absence of convulsions, pectoral flapping, and touch responses were recorded daily from the day after exposure to 5 dpf. (B) Apparatus used to assess startle responses to auditory/vibrational stimuli. A speaker with a bonded platform was sent a 3-ms, 1,000-Hz pulse, which was then delivered to a 16-well plate. A high-speed camera captured startle responses at 1,000 frames per second. (See the section “Equipment” in the Supplemental Material.) (C) Sample trace of the bend angle over time as a larva undergoes startle. Bend angle is estimated by measuring the changes in angles between three line segments that outline the larvae.

successful if there was a visible displacement of blood cells. Incorrectly injected fish (evidenced by morphological defects such as yolk punctures) were immediately removed from the study. The specific doses, injection times, and numbers of fish used in each experiment are indicated in the figure legends and associated tables and summarized in Table S1.

Assessment of Acute Neurotoxic and Morphological Phenotypes Associated with Developmental Exposure to DomA

Fish were imaged using brightfield microscopy to visualize potential gross morphological defects. The presence or absence of the swim bladder at 5–7 dpf was scored blindly, and then the percentage was quantified for fish exposed to DomA at different doses and during different developmental stages. Images were white balance-corrected using Adobe Photoshop.

To analyze morphological defects and acute neurotoxicity, fish were kept individually in 48-well plates for phenotypic observation. Mortality, the presence or absence of convulsions, pectoral flapping, and touch responses were recorded daily from the day after exposure to 5 dpf. Larvae were considered convulsing when whole body contractions were observed. Pectoral fin flapping was scored when larvae continued to rapidly move pectoral fins even when the fish were not active. Touch responses were assessed using a tactile stimulus produced by an embryo poker—a piece of fishing line (0.41-mm diameter). Larvae were identified as having no touch response when they were unable swim away following tactile stimulation.

Modeling the Prevalence of Neurotoxic Phenotypes by Dose, Day of Exposure, and Day of Observation

Following daily observation, generalized estimating equations (GEEs) were used to model the effects of both DomA dose (as a continuous factor) and the number of days postexposure (categorical factor) on the prevalence of acute neurological phenotypes [presence of convulsions or pectoral fin flapping (combined), lack of touch responses] within a trial [gee(); geepack R package] (version 3.6.1; R Development Core Team) (Højsgaard et al. 2006). Observations of the same group of fish over multiple days were treated as repeated measures.

There were only single observations for fish exposed at 4 dpf (observed at 5 dpf). To determine whether DomA dose alters the presence of neurotoxic phenotypes 1 d postexposure, a generalized linear model was formulated containing the different doses as predictors, and the prevalence of phenotypes within the treatment group as the response. To account for variability amongst trials, dispersion was estimated using the quasibinomial link function.

Startle Behavior Setup and Assessment (7 dpf)

The custom-built startle behavior setup (see the section “Equipment” in the Supplemental Material) is shown in Figure 1B. A speaker was connected to an amplifier, which served as a source of auditory/vibrational (A/V) stimuli. A hollow cylinder with a flat base was glued to the center of the speaker, and served as a platform to rest the plate that contained the fish (radius = 50 mm, height = 50 mm). A 16-well acrylic plate (4.83 × 4.83 cm) housed 16 larvae individually (Wolman et al. 2011). The intensity and frequency of the A/V stimuli were controlled using a pulse generator. Stimuli were coded to deliver 3-ms pulses of 1,000 Hz frequency (Matlab File 1).

Larvae were transferred to a light box beside the behavioral arena at least 5 min prior to testing. To assess startle, groups of 16 larvae (7 dpf) were given 7 identical stimuli (41 dB) that were spaced 20 s apart to prevent habituation (Wolman et al. 2011). A

high-speed video camera (Edgetronic) was set at a 10% pre-trigger rate to capture 13 frames prior to the stimulus being elicited, while recording larval movements at 1,000 frames per second.

All exposed larvae, including those with uninflated swim bladders, were tested. Any fish with overt morphological defects (those with opaque brains or with widespread edema) were excluded from the analysis.

Measuring startle vibration. Vibration was measured using a 3-axis accelerometer. The output signal was first conditioned and then passed through an analog filter using a 10-kHz low-pass cut-off frequency and 30 dB gain. Finally, the signal was collected by a data acquisition board. Raw voltage data were converted into acceleration units (meters per second squared) using manufacturer sensitivity values for each axis of the accelerometer. The Euclidian norm (vector sum) for the three acceleration signals was calculated to get the total acceleration. Individual peaks were identified, and metrics were calculated for the time window between 9 ms prior to the peak to 50 ms after. The maximum value (peak) during each time window was taken as the zero-to-peak acceleration value for a given impulse, and this value was converted to dB using the following equation:

$$L_{z-pk} = 20 \times \log_{10}(x),$$

where L_{z-pk} is the zero-to-peak acceleration level in dB re 1 m/s², and x is the maximum acceleration level (of the Euclidian norm) over the peak analysis window.

Startle Behavioral Analysis

High-speed videos were converted into JPEGs (.mov files with a minimal resolution of 720 × 720 pixels) (Matlab File 2). To reduce the noise and tracking errors, the background was subtracted, and the image contrast was enhanced using a custom script in MATLAB (Matlab File 3). Flote software was then used to analyze the JPEGs (Burgess and Granato 2007). Quantitative attributes of the startle response measured include startle responsiveness (whether larvae responded or not), latency (delay time prior to startle), maximal bend angle, and maximal angular velocity (Mav) during startle. The identities of individual larvae across the multiple stimuli were distinguished based on their position on a grid.

Statistical Modeling of Startle Responsiveness

Every fish was given seven replicate A/V stimuli, spaced 20 ms apart. For all instances where a fish was successfully tracked, response rates were recorded. Percent response rates for individual fish were calculated (percentage responsiveness = number of times the fish responded/number of successfully tracked videos with a maximum of seven tracks per individual fish). A mixed-effects logistic regression model was used to identify treatment differences in percent responsiveness, with dose as a fixed effect and the population of exposed fish (those exposed during a specific experimental trial) as a random effect [glmer(); lme4 R package] (Bates et al. 2015). A Dunnett post hoc test was used to identify potential treatment differences in responsiveness [glht(); multcomp R package] (Hothorn et al. 2008).

Identifying short latency C-bend vs. long latency C-bend Responses Using Mixture Models

For fish that responded, startle responses were classified as either short latency C-bends (SLCs) or long latency C-bends (LLCs). Latency cutoffs have been known to vary based on environmental conditions such as temperature (Burgess and Granato 2007). To

empirically determine the latency cutoffs, clustering was done using a Gaussian mixture model, which fits two Gaussian distributions, and assigns each latency data point a probability of belonging to either of the two distributions (R package, *mixtools*) (Benaglia et al. 2009). The cutoff for assigning a response as an SLC was 13 ms—the latency with a greater than 50% probability of belonging to the first fitted Gaussian distribution (Figure S1). Startle responses with latencies greater than 13 ms were classified as LLCs.

Analysis of Treatment Differences in Startle Response Kinematics

There were several instances when individual fish performed a combination of LLC and SLC responses over the seven replicate stimuli. Kinematic responses from the two types of startle responses (SLC vs. LLC) were analyzed separately based on previous research that shows they are driven by different neural circuits and have distinct kinematic characteristics (Burgess and Granato 2007; Marsden and Granato 2015; O'Malley et al. 1996). Following this classification, the median response of individual fish for each startle type was then used to identify treatment-specific differences in kinematics. The median response was analyzed in order to address potential outliers in the data that result from fish that were incorrectly tracked or were performing spontaneous movements unrelated to startle.

Normality and variance homogeneity were tested using the Shapiro-Wilk method [*shapiro.test()*, R] and Bartlett's test [*bartlett.test()*, R], respectively. Kinematic data (bend angle, maximum angular velocity) showed departures from normality and had unequal variances. To account for this, we used nonparametric tests to determine whether fish exposed to various doses of DomA at different developmental periods had altered bend angles and Mavs.

Kinematic data from fish exposed to DomA at different development days and during different experimental trials were analyzed separately. For trials that contained a single dose of DomA, nonparametric Behrens-Fisher *t*-tests were used to test the alternative hypothesis that kinematics of fish exposed to DomA were different from their control counterparts [*npar.t.test()*; *nparcomp* package, R] (Konietschke et al. 2015). For trials that contained multiple doses, we used a nonparametric multiple comparison procedure with Dunnett-type contrasts to compare each of the doses to the control [*nparcomp()*; *nonparam* package, R] (Konietschke et al. 2015; Munzel and Hothorn 2001). Both the nonparametric Behrens-Fisher *t*-tests and the nonparametric multiple comparison procedure with Dunnett-type contrasts compute relative effects, which range from 0 to 1. Under the null hypothesis, the relative effect size is 0.5, which represents a 50% probability (an equal probability) that the treated fish has a value greater than the control fish, whereas values closer to 0 indicate a higher probability that the measured kinematic parameter in the treated group has a smaller value than the control. After analysis of the individual trials, the responses of individual fish from different trials were then graphed together, with the fraction above each treatment (by day injected and dose) corresponding to the number of trials that showed statistically significant results.

Startle Kinematic Analysis for Interaction Effects between Dose and Day of Exposure

We directly tested whether there was an interaction between dose and day injected by analyzing a subset of trials that had fish that were collected from the same breeding cohort at 0 dpf and then exposed to DomA at different developmental days (1, 2, or 4 dpf). We assessed the kinematics of LLC startles because these

responses were shown by the previous analysis to be more sensitive to treatment differences.

Either a two-factor analysis of variance (ANOVA) or an aligned ranked transformed ANOVA test was done to determine whether there was an interaction between dose (0 vs. 0.09 ng, or in a separate analysis, 0 vs. 0.13 ng DomA) and day of exposure (1, 2, or 4 dpf) on startle kinematics [*aov()*, base R stats package *art()*; ARTool R package] (version 3.6.1; R Development Core Team) (Wobbrock et al. 2011).

An aligned ranked transformed ANOVA rather than a two-way ANOVA was used when there was heterogeneity of variance between treatment groups [assessed using Levene's test, *levTest()*], and model residuals from the two-factor ANOVA test were not normally distributed [assessed using the Shapiro test, *shapiro.test()*; base R base stats package] (Fox and Weisberg 2018).

Following the two-way ANOVA, Tukey's post hoc test was done to identify significant differences in kinematics between different treatment groups. Conversely, following aligned ranked transformed ANOVA, difference-of-difference contrast tests were performed to determine whether day of exposure affected the extent of kinematic differences between control and DomA-exposed fish. Nonparametric Mann-Whitney *U* tests were also employed to test for treatment differences within a specific day of exposure (e.g., comparing control with DomA-exposed fish injected at 1 dpf). The Holm-Bonferroni method was used to correct for multiple comparisons [*testContrasts()*; *Phia* R package] (Rosario-Martinez and Fox 2015).

Assessment of Startle Kinematics in Fish with Different Morphological Traits

To assess the effect of morphological phenotypes on startle kinematics, we reanalyzed a subset of trials in which fish were exposed to 0.14 ng of DomA at 2 dpf (3 trials). Morphological attributes (presence vs. absence of an inflated swim bladder; bent vs. straight body axis) were identified for individual fish from the kinematics videos. These morphological attributes were then matched to previously calculated startle kinematic measurements (outlined in the startle behavioral analysis section). A nonparametric multiple comparison procedure with Dunnett-type contrasts was used to determine whether DomA-exposed fish with different morphological attributes were different from control fish with control-like phenotypes—fish with inflated swim bladders and straight body axes [*nparcomp()*; *nonparam* package, R] (Konietschke et al. 2015; Munzel and Hothorn 2001).

Fluorescence Microscopy

Fluorescence microscopy was used to image transgenic fish (see below). Fish were anesthetized in MS222 (0.16%) and then imaged using either widefield epifluorescence microscopy or confocal microscopy. For images collected on the confocal microscope, fish were mounted laterally in 1.5% low-melt agarose and imaged using the confocal microscope with the 40× water objective [numerical aperture (NA) = 1.1]. Images were taken along the anterior spinal cord in the region around the 5th and 10th somites.

For rapid imaging on the widefield epifluorescence microscope, fish were oriented into custom-made acrylic molds that contained narrow channels; anesthetized larvae were positioned laterally using the embryo poker. Fish were imaged using an inverted epifluorescence microscope with either a 20× (Fluar, NA = 0.75) or a 10× (Fluar, NA = 0.5) objective. Images were taken along the anterior to medial spinal cord between somites 5 and 15.

Analysis of the Prevalence and Severity of Myelin Phenotypes by Dose and Day of Exposure

Tg(mbp:EGFP-CAAX) is a stable line in which EGFP is localized to myelin sheaths (Almeida et al. 2011). We exposed *Tg(mbp:EGFP-CAAX)* fish to different doses of DomA at selected developmental times (Figure 1A) and then imaged their spinal cords using fluorescence microscopy.

We first assessed myelin defects at 5- to 7-dpf in fish exposed to intermediate doses (0.13–0.14 ng) of DomA at 1, 2, and 4 dpf. Once we determined that exposure to 0.14 ng DomA at 2 dpf resulted in myelin defects, we then sought to narrow the defined window of susceptibility by assessing myelin integrity following exposures at 1, 2, 2.5, 3, and 4 dpf. We further tested a more extensive range of doses of DomA (0.09, 0.13, 0.14, and 0.18 ng) with exposure at 2 dpf.

Images were blindly classified qualitatively into Categories 0–5 based on the severity in the myelin defects observed (Figure S2). The categories and descriptions were as follows: (0) Normal phenotype—dorsal and ventral regions had labeled myelin sheaths. The myelin sheath surrounding the Mauthner axon was visible. (1) Myelin sheaths were present but disorganized. In some cases, myelinated axons that were normally found ventrally were located more dorsally. In others, the myelinated axons terminated prematurely with distal ends located more dorsally. (2) Myelin was labeled in both the dorsal and ventral regions of the spinal cord, but there were some deficits. Although the ventral spinal cord was labeled, it had noticeably less myelin labeled compared with controls. (3) The loss of labeled myelin in the ventral spinal cord resulted in large, observable gaps between myelinated axons. (4) Myelin was essentially nonexistent in the ventral spinal cord. Instead of sheaths forming, numerous hollow circular profiles were present both in the ventral and dorsal spinal cord. (5) Visible sloughed off portions of myelin were defined by a rough-looking appearance and being separated from the thin elongated sheaths.

Multinomial logistic regression was used to model the effect of both dose and day injected on the distribution of the myelin severity phenotypes [multinom(); nnet R package] (Venables and Ripley 2002).

The overall significance of the dose and development day of exposures was obtained by performing a drop-in-deviance test to compare residual deviances from two multinomial logistic regression models. Model 1 included the dose of DomA as a predictor of the distribution of myelin phenotypes: $\beta_0 + \beta_{\text{dose}}$. Model 2 incorporated both dose and day of exposure: $\beta_0 + \beta_{\text{dose}} + \beta_{\text{DayExposure}}$. A drop-in-deviance test was then used to determine whether the more complex Model 2 was significantly better at capturing the data than the initial simpler one [ANOVA (initial model, first alternative model), car package, R] (Fox and Weisberg 2018).

Multinomial logistic regression models were constructed to identify the effects of increasing doses of DomA injected at 2 dpf on the distribution of these myelin phenotypes.

Time-Lapse Microscopy

Tg(nkx2.2a:mEGFP) × Tg(sox10:RFP) embryos were exposed to DomA (0.14 ng; $n = 6$) or the vehicle saline ($n = 5$) at 2 dpf. At approximately 2.25 dpf, they were anesthetized and mounted in 1.5% low-melt agarose. Images were acquired on the LSM710 using the 20× dry (Plan-Apochromat 20×/0.8) objective. Z-stacks were acquired every 9–13 min over the course of 12–13 h. For each embryo observed, maximum intensity projections of the z-stacks were then generated and compiled over time to generate the movie file (ZEN blue, ZEN black imaging software, Zeiss Microscopy).

Experimental Design for RNA-seq

Three individual breeding tanks were set up with two male and one female *Tg(mbp:EGFP-CAAX)* adults per tank. Embryos

collected from each tank were split so that some were injected with DomA (0.14 ng) and others with the saline vehicle control. The dose (0.14 ng) was chosen because the previous experiments showed that exposure to this dose led to consistent behavioral and structural phenotypes without leading to other broad-scale neurotoxic effects. Stratified random sampling was employed by selecting embryos randomly within three 15-min injection blocks, with injections taking place over a 2-h span. This was to ensure that there would be no potential confounding from the timing of injections over the 2-h time span. Pools of six embryos from each of the three breeding sets were collected for RNA sequencing (RNA-seq; $n = 3$ pools of six embryos per treatment) at 3 dpf (76 hpf). The remaining fish were used for imaging myelin at 5 dpf and for assessing startle behavior at 7 dpf (see below). At the end of the behavioral trial, a subset (3 pools of 6 larvae per treatment) of the fish was snap frozen at 7 dpf (124 hpf) for RNA-seq. Two DomA-exposed embryos were excluded from the RNA-seq experiment because these larvae had no visible acute phenotypes immediately postinjection (at 2 dpf) and showed no myelin defects at 5 dpf.

To ensure effectiveness of the exposure, exposed fish were imaged to visualize myelin structure at 5 dpf and then subjected to behavioral tests (startle response) at 7 dpf. Phenotypic analysis thus validated the use of RNA-seq to identify potential transcriptional changes from exposures.

RNA Isolation and Sequencing

RNA was isolated using the Zymo Direct-Zol kit (ZymoResearch) and quantified using a Nanodrop spectrophotometer. RNA quality was checked using the Bioanalyzer (Harvard Biopolymers Facility, Cambridge, MA). RNA integrity numbers were ≥ 8.2 . Library preparation for single stranded RNA-seq was done using the Illumina TruSeq total RNA library kit. Single-end 50 base pair sequencing was done on an Illumina HiSeq2000 platform. Library preparation and sequencing were performed at the Tufts University Core Facility (Boston, MA). Raw data files were assessed for quality using FastQC (Andrews 2010). Adapter trimming was done using Trimmomatic (Bolger et al. 2014). Trimmed reads were aligned to the genome (GRCz10, version 84) using Spliced Transcripts Alignment to a Reference (STAR) software (Dobin et al. 2013). HTSeq-count was used to count the number of reads mapped to the annotated regions of the genome (Anders et al. 2015). Differential gene expression (DGE) analysis was done using Bioconductor package, edgeR, following the DGE analysis pipeline of Chen (Chen et al. 2016; Robinson et al. 2010). Raw and processed data files were deposited in National Center for Biotechnology Information Gene Expression Omnibus database (accession no. GSE140045).

DGE analysis involved filtering genes with read counts less than $10/n$, where n is the minimal library size, and then normalizing read counts. Negative binomial models were used to account for gene-specific variability from biological and technical sources. Multidimensional scaling (MDS) plots were used to visualize the leading fold changes (largest 500 \log_2 fold changes) between pairs of samples. False discovery rate of 5% [Benjamini-Hochberg method (Benjamini and Hochberg 1995)] was used as a statistical cutoff for identifying differentially expressed genes. Gene annotation was done using BioMart with GRCz11. gProfiler (version r1750_e91_eg38) was then used to identify enriched Gene Ontology (GO) terms and human phenotype ontology terms (Köhler et al. 2019; Reimand et al. 2016). GO terms with evidence only from *in silico* curation methods were excluded from the enrichment analysis and a statistical significance level of ≤ 0.05 (adjusted p -value using the g:SCS threshold) was used.

Results

To elucidate the developmental windows of susceptibility to DomA and explore the mechanisms involved, we established a zebrafish exposure model involving intravenous injection of DomA into embryos or larvae at discrete developmental periods ranging from 1 and 4 dpf. The molecular, cellular, and behavioral end points were assessed at later times (3–7 dpf) (Figure 1A).

Gross Morphological Effects from Developmental Exposure to DomA

We initially examined acute effects resulting from DomA exposure over a range of doses. A majority of the larvae exposed to DomA at 2 dpf did not have inflated swim bladders at 5 dpf (Figure S3A,B; Table S2). Furthermore, some larvae injected at 4 dpf with the highest dose of DomA (0.18 ng) had brains with a darkened appearance. These opaque brains were signs of widespread apoptosis or necrosis, suggesting that this dose could lead to widespread neurotoxicity (Table S3). Based on this, DomA doses of 0.14 ng or lower were primarily used for imaging and gene expression analyses.

Acute Neurotoxic Phenotypes Associated with Developmental Exposure to DomA

Injection of DomA at low doses (0.09–0.14 ng) caused transient, acute effects that included the loss of touch responsiveness, pectoral flapping, and convulsions (Figure S3C,D; Tables S5–S9). These resolved within 1 d of exposure and did not lead to appreciable mortality (Table S4). Specifically, the percent of fish displaying touch responsiveness/response was significantly lower in the DomA-treated fish exposed at 1 and 2 dpf (0.09–0.18 ng) compared with their respective controls (Figure S3C; Tables S5, S6, and S8). The prevalence of this phenotype increased with the dose of DomA ($p = 1.54 \times 10^{-8}$ for 1 dpf injected; $p = 9.4 \times 10^{-9}$ for 2 dpf), but was transient, dropping significantly after the first day postexposure ($p = 0.0028$ for 1 dpf, $p = 5.9 \times 10^{-6}$ for 2 dpf). In contrast, for exposures at 4 dpf, no fish exposed to DomA doses <0.14 ng exhibited any touch response deficits and nearly all of the fish with touch response deficits were in the group exposed to the highest DomA dose (0.18 ng) (Table S7).

Similarly, fish exposed to DomA at both 1 and 2 dpf (but not at 4 dpf) had a dose-dependent increase in the prevalence of convulsions or pectoral fin flapping ($p = 0.0001$ for 1 dpf-exposed fish, $p = 3.9 \times 10^{-7}$ for 2 dpf-exposed fish) (Figure S3D; Tables S5–S7 and S9). This phenotype was also transient, dropping significantly after 1–2 d postexposure ($p = 0.001$ for 1 dpf-exposed fish comparing prevalence at 3 d postexposure to a day after exposure, $p = 2.2 \times 10^{-9}$ for 2 dpf-exposed fish comparing prevalence 2 d postexposure to a day after exposure) (Figure S3D; Tables S5 and S9). Although fish exposed to DomA at both 1 and 2 dpf exhibited convulsions or pectoral fin flapping, 2 dpf-exposed fish exhibited these acute neurotoxic phenotypes at higher proportions, especially at the higher doses (0.14–0.18 ng) (Tables S5, S6, and S9).

Startle Responsiveness to A/V Stimuli after Developmental Exposure to DomA

We assessed the functional impact of developmental DomA exposure by measuring startle response behavior during the larval stage (7 dpf) of development. We first assessed responsiveness—the ability of fish to react to A/V stimuli. Fish exposed to DomA at 2 dpf were significantly less responsive to A/V stimuli at all doses tested (0.09–0.18 ng) ($p < 0.001$) compared with controls (Figure 2; Table S10). In contrast, fish exposed to DomA at 1 dpf were less responsive only when exposed to doses ≥ 0.13 ng ($p \leq 0.001$), whereas those exposed to DomA at 4 dpf were significantly less responsive only when exposed to the highest dose (0.18 ng) tested ($p < 1 \times 10^{-4}$).

Startle Response Kinematics after DomA Exposure

During the larval startle response, larvae perform a distinctive C-bend as the head and body bend together at a high angular velocity (Figure 1C; Video S1). Kinematics that underlie this C-bend include bend angle and Mav. We evaluated kinematics for the two types of startle responses: SLC and LLC startle responses (Figure S1).

Exposure to DomA at 2 dpf led to consistent kinematic deficits at all doses tested and in all experimental trials (Figures 3 and 4; Tables S11–S13). Fish exposed to DomA at 2 dpf had both smaller bend angles and slower Mavs relative to vehicle-

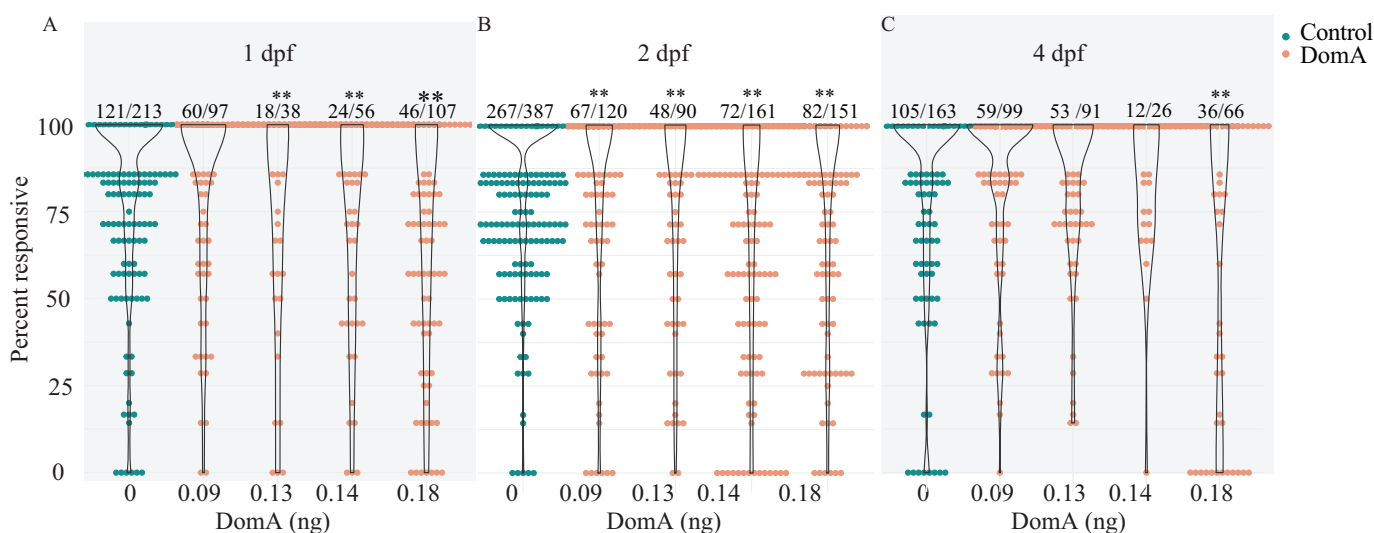


Figure 2. Startle responsiveness in zebrafish exposed to domoic acid (DomA) at 1, 2, and 4 d postfertilization (dpf). Fish were exposed to different doses of DomA at (A) 1 dpf, (B) 2 dpf, or (C) 4 dpf, and startle responses were measured at 7 dpf. Points represent the percentage response of individual fish to replicate stimuli. Ratios listed above represent the number of fish that responded to 100% of the stimuli over the total number of fish tested per treatment group. Violin plots are overlaid to show kernel density distribution of the data. Significance was determined with post hoc pairwise Dunnett comparisons following binomial modeling of percentage responsiveness. p -Values indicate significant differences in responsiveness in DomA-exposed larvae compared with controls injected with saline during the same developmental time period (*, $p < 0.05$; **, $p < 0.005$). Responsiveness data from nine trials were combined. See Table S10 for data.

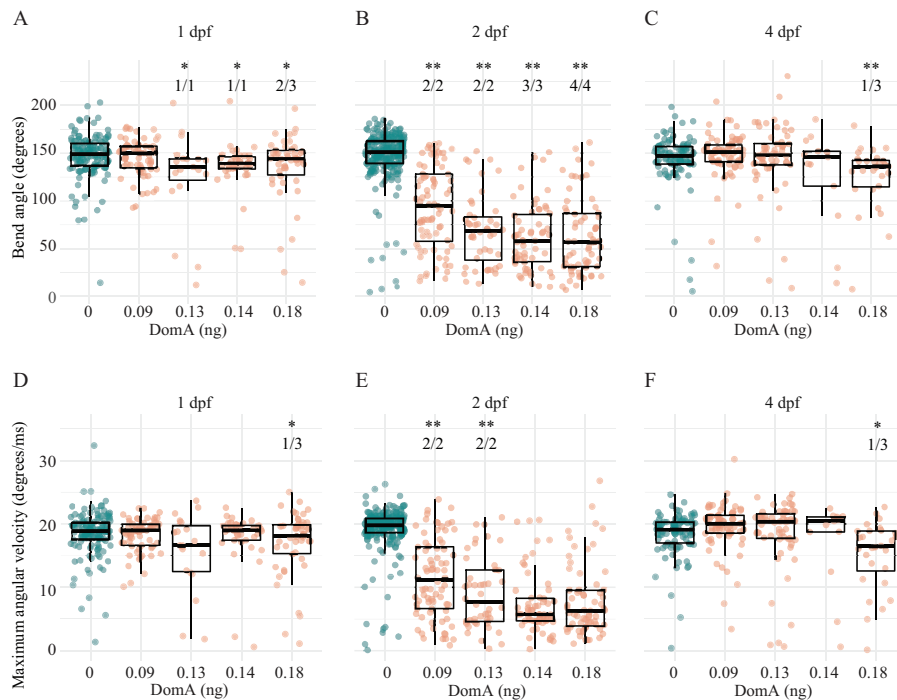


Figure 3. Kinematics for short latency C-bend (SLC) startles in zebrafish exposed to domoic acid (DomA) at 1, 2, and 4 d postfertilization (dpf). Fish were exposed to different doses of DomA at (A,D) 1 dpf, (B,E) 2 dpf, and (C,F) 4 dpf, and startle responses were measured at 7 dpf. SLC startle responses were characterized by (A–C) bend angle and (D–F) maximal angular velocity. Each point represents the median of up to seven responses for an individual fish. Box plots show the group medians, upper 75% quantiles, and lower 25% quantiles. Significance was determined using Behrens-Fisher *t*-tests (for trials with one DomA dose) or using nonparametric multiple comparison procedures with Dunnett-type contrasts (for trials with multiple DomA doses). Asterisks represent statistical significance between DomA and controls within a single trial (*, $p < 0.05$; **, $p < .001$). The numbers shown above each column represent the number of trials with statistically significant treatment effects/the total number of trials conducted. Tables S11, S14, and S16 contain the results from the statistical analysis for 2 dpf-, 1 dpf-, and 4 dpf-injected fish, respectively. Table S13 includes medians and interquartile ranges for 2 dpf-injected fish.

injected controls; these behavioral deficits were evident with both SLC (Figure 3; Tables S11, S13) and LLC startle responses (Figure 4; Tables S12 and S13).

In contrast to exposure at 2 dpf, exposure at 1 and 4 dpf to the lowest dose of DomA tested (0.09 ng) did not lead to any kinematic deficits for either type of startle (SLC or LLC) (Figures 3 and 4; Tables S14 and S15). At higher doses (0.13–0.18 ng), exposure to DomA at 1 dpf led to kinematic deficits that differed by startle response type. Fish exposed to DomA (≥ 0.13 ng) at 1 dpf had smaller bend angles and slower Mavs, particularly when they performed the LLC startle responses (Figure 4). These fish also had significant kinematic deficits when performing the SLC responses, but this was primarily in smaller bend angles rather than slower Mavs (Figure 3; Table S15). Exposures to DomA at 4 dpf did not result in consistent effects on kinematics (Figures 3 and 4; Tables S16 and S17). Thus, although exposures to DomA at all developmental stages tested (1, 2, and 4 dpf) resulted in some kinematic deficits in all trials, only those at 2 dpf consistently led to kinematic deficits in all trials and across the entire range of doses tested.

We then directly compared the effect of both dose and day of exposure on LLC startle kinematics using trials in which fish from the same breeding cohort were exposed to DomA at 1, 2, and 4 dpf.

At the lowest dose of DomA (0.09 ng), startle kinematic parameters were significantly influenced by the interaction between treatment and day of exposure for bend angle [$F(2, 520) = 21.6$, $p = 1 \times 10^{-9}$] and for Mav [$F(2, 520) = 14.7$, $p = 6.2 \times 10^{-7}$] (Figure S4A,C). Treatment effects from exposure to DomA at 2 dpf were distinct from treatment effects from exposures at 1 dpf ($p = 8.7 \times 10^{-8}$) or 4 dpf ($p = 8.7 \times 10^{-8}$). Although fish exposed to DomA at 2 dpf had significantly lower Mavs ($p = 1 < \times 10^{-10}$) and smaller bend angles ($p = 5.91 \times 10^{-11}$) compared with their control counterparts, those exposed at 1 dpf and at 4 dpf had

indistinguishable bend angles (1 dpf: $p = 0.97$, 4 dpf: $p = 0.79$), and Mavs (1 dpf: $p = 0.97$, 4 dpf: $p = 0.99$) compared with their controls. Thus, at the lowest doses of DomA (0.09 ng), exposure at 2 dpf led to distinct kinematic deficits that were not found when exposures occurred 1 or 4 dpf.

With exposure to the intermediate doses of DomA (0.13–0.14 ng), the interaction between treatment and day of exposure remained significant for both bend angle [$F(2, 474) = 23.0$, $p = 3 \times 10^{-10}$] and Mav [$F(2, 474) = 19.2$, $p = 9.2 \times 10^{-9}$] (Figure S4B,D). Similar to the results with the lowest dose of DomA, exposure to 0.13 ng DomA at 2 dpf led to significant kinematic deficits relative to exposures at 1 dpf ($p = 4.4 \times 10^{-6}$) and at 4 dpf ($p \leq 0.0001$). In addition, fish exposed to intermediate doses of DomA at 1 dpf had smaller bend angles and slower maximum angular velocities relative to their control counterparts (bend angle: $p = 0.002$, Mav: $p = 0.008$). However, these deficits were less pronounced compared with those that occur after exposure at 2 dpf (bend angle comparison estimate for treatment effects between 1 and 2 dpf = -141) [$(p = 4.4 \times 10^{-6})$; Mav comparison of DomA-exposed fish at 2 vs. 1 dpf ($p < 1 \times 10^{-10}$)]. Thus, at medium doses of DomA, exposure at 1 dpf led to significant kinematic deficits. However, these were still less severe than when exposure occurred at 2 dpf.

Startle kinematics were determined for all exposed fish, including those with uninflated swim bladders. To address the possibility that the startle response deficits observed at 2 dpf were due only to morphological defects (uninflated swim bladders or bent body axes in a subset of fish with uninflated swim bladders), we reanalyzed three trials in which fish were exposed to 0.14 ng of DomA at 2 dpf—the treatment combination that led to pronounced behavioral deficits. DomA-exposed fish with uninflated swim bladders had more pronounced kinematic deficits than those with inflated swim bladders (estimated relative effect size of 0.042 vs. 0.094)

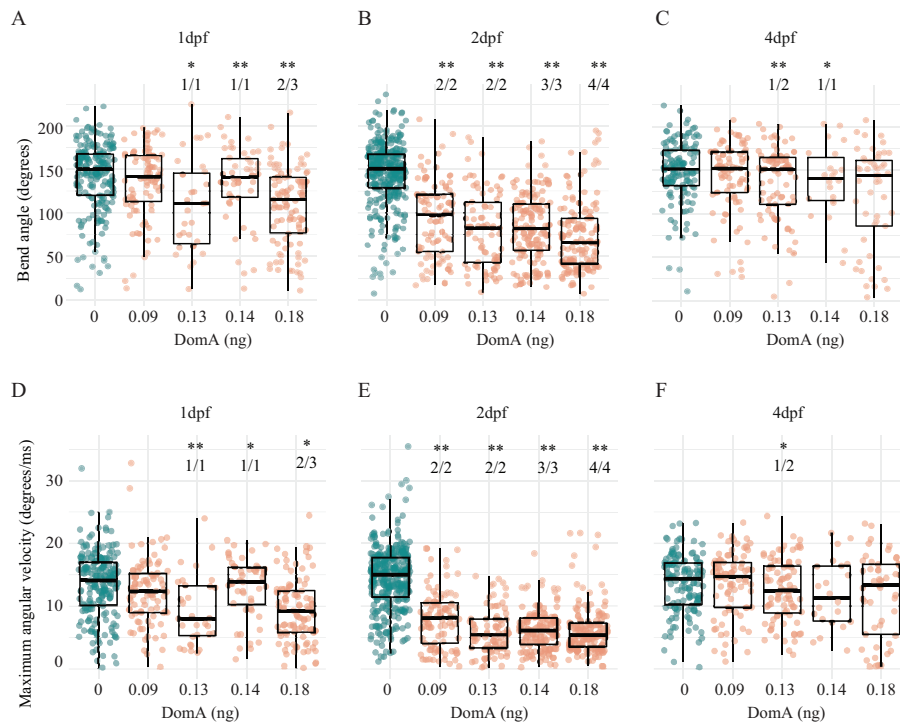


Figure 4. Kinematics for long latency C-bend (LLC) startles in zebrafish exposed to domoic acid (DomA) at 1, 2, and 4 d postfertilization (dpf). Fish were exposed to different doses of DomA at (A,D) 1 dpf, (B,E) 2 dpf, and (C,F) 4 dpf, and startle responses were measured at 7 dpf. LLC startle responses were characterized by (A–C) bend angle and (D–F) maximal angular velocity. Each point represents the median of up to seven responses for an individual fish. Box plots show the group medians, upper 75% quantiles, and lower 25% quantiles. Significance was determined using Behrens-Fisher *t*-tests (for trials with one DomA dose) or using nonparametric multiple comparison procedures with Dunnett-type contrasts (for trials with multiple DomA doses). Asterisks represent statistical significance between DomA and controls within a single trial. (*, $p < 0.05$; **, $p < .001$). The numbers shown above each column represent the number of trials with statistically significant treatment effects/the total number of trials conducted. Tables S12, S15, and S17 contain the results from the statistical analysis for 2 dpf-, 1 dpf-, and 4 dpf-injected fish, respectively. Table S13 includes medians and interquartile ranges for 2 dpf-injected fish.

(Figure S5A,B; Table S18). This was also true for DomA-exposed fish with bent body axes vs. those that had straight body axes (Figure S5C,D; Table S19). Nonetheless, DomA-exposed fish with normal morphologies (fully inflated swim bladders and straight body axes) still had kinematic deficits compared with control fish (Figure S5; Tables S18 and S19).

Myelination in the Spinal Cord after DomA Exposure

Startle response deficits could arise from myelin defects. Proper myelination in the spinal cord is critical for rapid startle responses, and mutations that disrupt myelin structure cause lower angular velocities, shallower bend angles, and longer startle latencies (Pogoda et al. 2006). To determine whether disrupted myelination underlies the DomA-induced deficits in startle response, we exposed fish with labeled myelin sheaths [*Tg(mbp:EGFP-CAAX)*] (Almeida et al. 2011) to a range of DomA doses and then assessed spinal cord myelination during the larval stages (Figure 5A).

Exposed fish were imaged at 5 dpf using confocal microscopy (Figure 5B). The severity of myelin defects was scored blindly on the scale of 0–4 (Figure 5D; Figure S2). Exposure to DomA caused myelin sheath defects, with the prevalence and severity influenced by day of exposure (Figure 5B,C; Table S20). Fish exposed to DomA at 1 dpf had no visible myelin defects ($n = 31$). In contrast, 32% of fish exposed at 1.5 dpf had visible myelin defects ($n = 11$ of 34). Defects included the overall reduction in labeled myelin, along with the appearance of unusual circular membranes (Figure 5B). The majority of fish (91%) exposed at 2 dpf showed myelin defects ($n = 96$ of 106). The prevalence of these defects remained high for fish exposed at 2.5 dpf, with 35 of 40 (88%) exhibiting a myelin defect. However, these myelin

phenotypes were less severe, with 2.5 dpf-exposed larvae having milder myelin sheath defects compared with those exposed to 2 dpf. In comparison, very few fish exposed to DomA at 4 dpf had disrupted myelin sheaths ($n = 2$ out of 46).

Confocal imaging data suggested that fish exposed at 2 dpf had more severe and more prevalent myelin defects compared with those exposed to DomA at other developmental periods. To confirm this, we performed additional experiments in which fish were exposed to DomA (at various doses and times) and then imaged at 5 dpf using widefield epifluorescence microscopy (Figure 6; Tables S21 and S22). This provided the higher throughput to statistically model the effects of DomA dose and the timing of exposure on the distribution and prevalence of the observed myelin sheath defects.

To determine whether the day of exposure influenced the appearance and prevalence of myelin defects, we performed a drop-in-deviance test to compare an initial model, with only DomA dose as the predictor, to an alternative model with both dose and day of exposure as predictors. Incorporating the day of exposure significantly improved the model's predictive power ($p < 1 \times 10^{-16}$), indicating that timing of DomA exposure influenced myelin deficits (Table S23).

We then determined whether DomA exposures (0.14 ng) that occurred during particular periods in development led to a higher prevalence of specific myelin defects at 5 dpf. We found that the odds of fish exhibiting myelin defects (those from Categories 1–4) were higher when exposures occurred at 2 dpf, relative to exposures that occurred at any other developmental period tested (1, 2.5, 3, and 4 dpf) (Table S24; $p < 1 \times 10^{-7}$ for 2 dpf exposed). Conversely, the odds of fish exhibiting a Category-5 myelin defect were higher when fish were exposed later in development

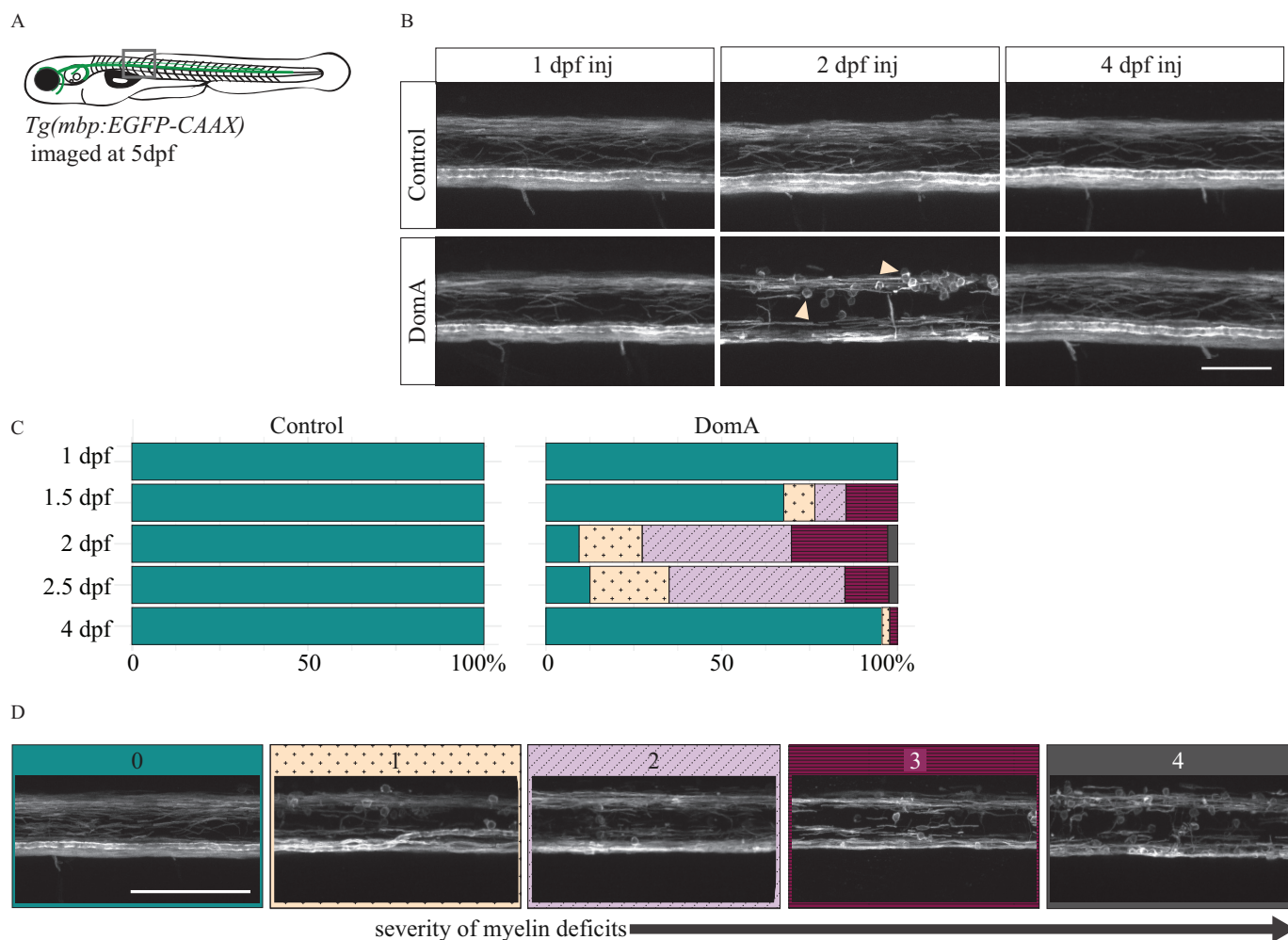


Figure 5. Confocal imaging of myelin sheath structures of zebrafish exposed to domoic acid (DomA) at different developmental days (A) *Tg(mbp:EGFP-CAAX)* fish were used to visualize labeled myelin sheaths. (B) Representative images of fish exposed to DomA (0.13–0.14 ng) during discrete periods in early development [1–4 d postfertilization (dpf)], then imaged at 5 dpf using confocal microscopy. Arrows indicate the unusual circular membrane profiles. (C) Stacked bar plots show the distribution of the different myelin phenotypes when fish were exposed to DomA at discrete developmental times. Multiple trials were combined to calculate the percentage distribution per phenotype observed. (D) Representative confocal microscopy images of different myelin phenotypes that were observed. Each fish was blindly classified and assigned a category based on the severity of the myelin deficit observed. The scoring was as described in detail in Figure S2. Briefly, the classification was as follows: (0) normal phenotype, (1) myelin sheaths present but disorganized, (2) myelin with noticeable deficits, (3) myelin gaps in ventral spinal cord, and (4) myelin sheaths lacking in ventral spinal cord. Scale bar: 50 μ m (Figure 5B) and 100 μ m (Figure 5D). Table S20 includes the number of trials represented along with the associated numbers of fish per trial.

(2.5–4 dpf) However, this phenotype was not prevalent, even at these later periods (Figure 6; Table S24).

To determine whether the myelin phenotypes observed at 5 dpf persist, fish were also imaged at 6 and 7 dpf (Figure 7; Tables S25–S28). Similar to imaging at 5 dpf, fish exposed to DomA at 2 dpf and then imaged at 6 or 7 dpf had a significantly higher incidence of myelin defects compared with control fish (Table S29). Furthermore, the higher the dose of DomA (delivered at 2 dpf), the more likely it was for the fish to exhibit all of the myelin phenotypes observed (Figure 7A,B; Tables S26, S28, and S29).

Effects of DomA on the Initial Stages of Myelin Sheath Formation as Revealed by Time-Lapse Imaging

We observed very few myelination defects or behavioral phenotypes in larvae exposed to DomA at 4 dpf, a time point after the onset of myelination. We hypothesized that, rather than affecting established sheaths, DomA is perturbing the formation of nascent myelin. To test this hypothesis, we imaged fish exposed to DomA at 2 dpf either during the initial stages of myelin formation, or

shortly after it. We found that DomA-exposed fish already had disrupted myelin sheaths by 3 dpf (the earliest development period at which myelin sheaths are established) (Figure 8A). To directly visualize the initial stages of myelin sheath formation, we performed time-lapse imaging in double transgenic fish (*Tg:sox10:RFP; Tg:nkx2.2a:mEGFP*), in which cells of the oligodendrocyte lineage—the cells responsible for myelination in the central nervous system (Czopka 2016)—are labeled. Imaging the axon wrapping and nascent myelin sheath formation from 2.5–3 dpf confirmed that all the control animals developed myelin ($n = 5$), whereas oligodendrocytes in all of the DomA-exposed larvae ($n = 6$) were unable to form elongated sheaths but, rather, formed unusual circular membranes (Figure 8B; Videos S2 and S3).

RNA-seq to Evaluate Gene Expression Changes after DomA Exposure

To identify the gene expression changes that accompany the myelination and startle deficits, whole-embryo RNA-seq was performed on embryos exposed to 0.14 ng DomA at 2 dpf and then sampled at

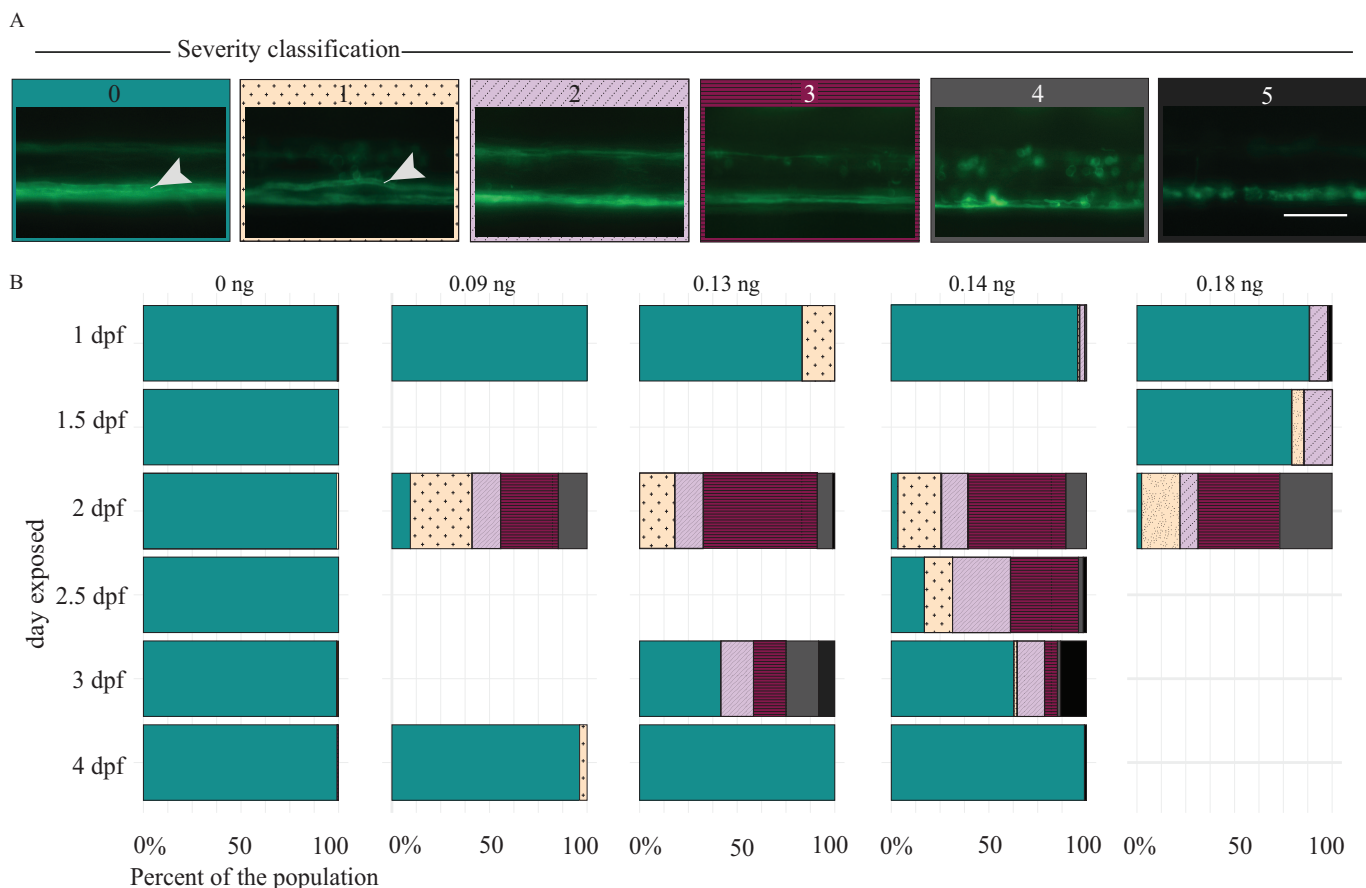


Figure 6. Myelin sheaths of zebrafish at 5 d postfertilization (dpf) following exposure to domoic acid (DomA) at different developmental days. (A) *Tg(mbp:EGFP-CAAX)* fish were exposed to DomA (0.09–0.18 ng) over a range of discrete developmental periods (1–4 dpf), then imaged at 5 dpf using widefield epifluorescence microscopy. Images were blindly classified into six categories based on the severity of the observed myelin phenotype. The scoring was as described in detail in Figure S2. Briefly, the classification was as follows: (0) normal phenotype, (1) myelin sheaths present but disorganized, (2) myelin with noticeable deficits, (3) myelin gaps in ventral spinal cord, (4) myelin sheaths lacking in ventral spinal cord, and (5) visible sloughed myelin. Arrows indicate the myelinated Mauthner axon that is required for short latency C-bends startle responses. (B) Stacked bar plots show the distribution of the different phenotypes. Multiple trials were combined to calculate the percentage distribution per phenotype observed. Scale bar: 50 μ m Table S21 includes the number of trials represented along with the associated numbers of fish per trial. Table S22 includes the myelin phenotype classification by dose and day injected. Table S24 contains the output of the multinomial logistic regression model to assess the role of developmental day of exposure on the distribution of myelin phenotypes. Table S29 contains the output of the multinomial logistic regression model for the influence of dose on the distribution of myelin phenotypes.

3 and 7 dpf (Figure 9A; Excel Tables S1 and S2). To ensure that the fish used for RNA-seq exhibited the same behavioral and cellular changes observed in other experiments, myelin sheath labeling was assessed at 5 dpf and startle response was assessed at 7 dpf in a subset of the exposed fish. The results confirmed the differences in behavior and myelin labeling between DomA-exposed fish and controls (Figure S6). Fish exposed to DomA at 2 dpf had shorter bend angles and slower angular velocities relative to controls (Figure S6A,B). Also consistent with other experimental trials, only DomA-exposed larvae showed any visible myelin defects, with most of the fish having myelin defects that were in the second to highest severity (Category 3 = 21/49; Figure S6C). Phenotypic analysis thus validated the use of RNA-seq to identify potential transcriptional changes from exposures.

RNA-seq yielded an average of 21 million raw reads per sample. Of these, 77.6% were uniquely mapped to the zebrafish genome. An MDS plot revealed that differences in gene expression were clustered primarily by both developmental stage (3 dpf vs. 7 dpf) and breeding clutch (3 breeding trios) (Figure 9B). However, a number of genes were identified as being differentially expressed in response to DomA.

Statistical analysis revealed differential expression of 82 genes at 3 dpf (28 h postexposure), and 10 genes at 7 dpf in DomA-

exposed fish vs. controls (Figure 9C,D; Tables S30 and S31; Excel Tables S1 and S2). Among the 82 genes differentially expressed at 3 dpf, 51 genes were down-regulated and 31 were up-regulated in DomA-exposed larvae as compared with controls.

Pathway analysis of the differentially expressed genes (DEGs; DomA vs. control; Excel Tables S1 and S2) indicated an overrepresentation of the GO biological process terms—protein depolarization and microtubule depolarization. The genes represented under these GO terms include genes in the stathmin family. Two of three stathmin genes were up-regulated, and one was down-regulated in DomA-exposed fish.

Human phenotype ontology terms that had a statistically significant association with the down-regulated genes included peripheral axonal degeneration, segmental peripheral demyelination/remyelination, and myelin outfoldings (Table S31). Several genes required for the maintenance of axonal structure (*neflb*, *nefmb*, *nefma*, *nefla*) (reviewed by Julien and Mushynski 1998; Yuan et al. 2012) and myelin structure (*mpba*, *mpz*) (reviewed by Barkovich 2000; Boggs 2006; Niemann et al. 2006) were down-regulated in DomA-exposed fish relative to controls and were overrepresented in the human phenotype ontology terms (Figure 10). There were no human disease phenotypes associated with up-regulated genes.

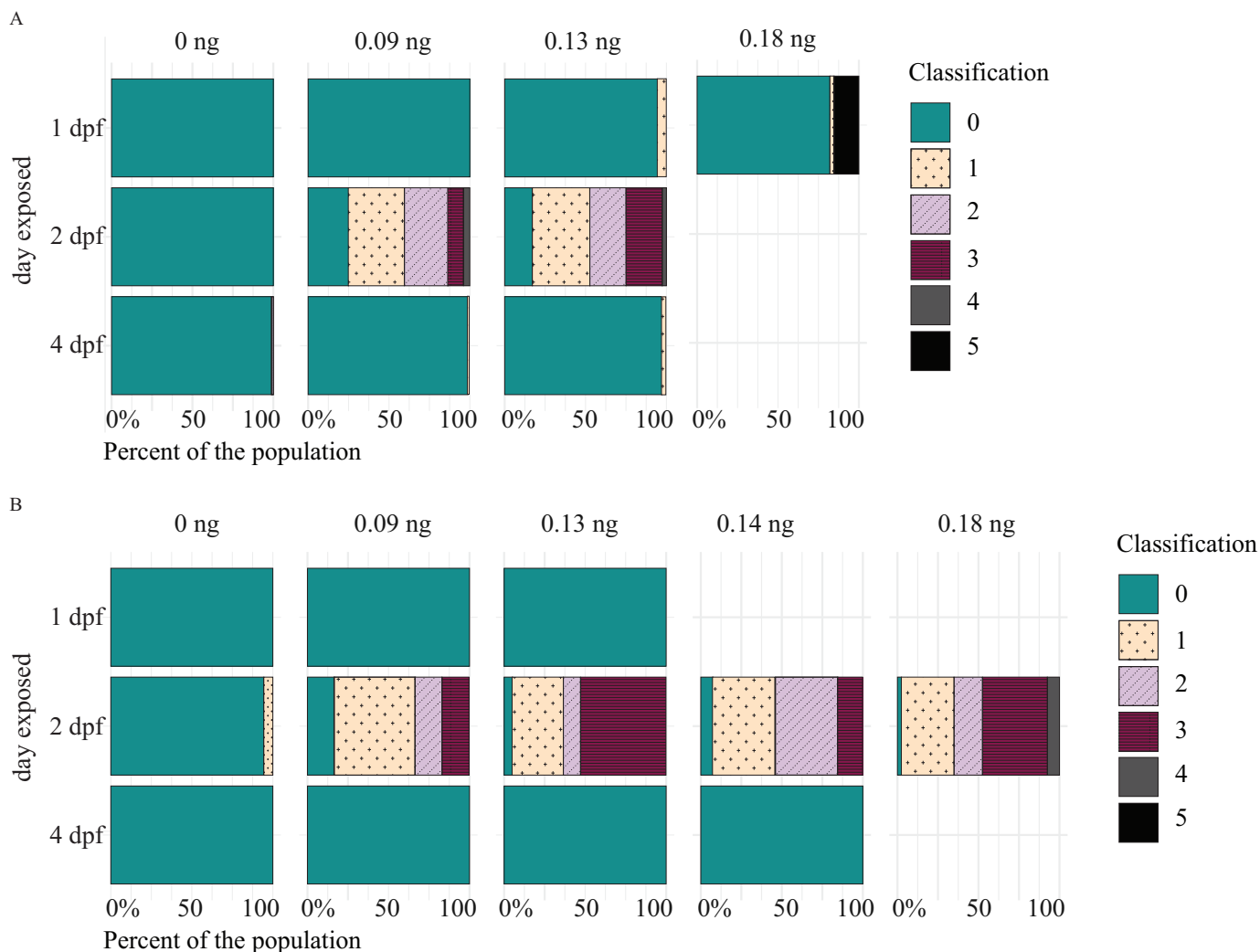


Figure 7. Myelin sheaths of zebrafish at 6 and 7 d postfertilization (dpf) following exposure to domoic acid (DomA) at different developmental days. *Tg(mbp:EGFP-CAAX)* fish were exposed to DomA over discrete developmental periods (1, 2, and 4 dpf), then imaged at (A) 6 dpf and (B) 7 dpf using widefield epifluorescence microscopy. Images were blindly classified into six categories based on the severity of the observed myelin phenotype. The scoring was as described in detail in Figure S2. Briefly, the classification was as follows: (0) normal phenotype, (1) myelin sheaths present but disorganized, (2) myelin with noticeable deficits, (3) myelin gaps in ventral spinal cord, (4) myelin sheaths lacking in ventral spinal cord, and (5) visible sloughed myelin. Stacked bar plots show the distribution of the different phenotypes per each dose. Data from individual fish from multiple trials were combined to calculate the percentage distribution per phenotype observed. Tables S25 and S27 contain the number of trials and associated numbers of fish per trial for 6 dpf- (A) and 7 dpf-injected fish (B), respectively. Table S26 includes myelin phenotype classification by dose and day injected, with imaging at 6 dpf. Table S28 includes myelin phenotype classification by DomA dose and day injected, with imaging at 7 dpf. Table S29 contains the output of the multinomial logistic regression model for the influence of dose on the distribution of myelin phenotypes.

At 7 dpf, there were only 10 DEGs, with 9 down-regulated and 1 up-regulated in DomA-exposed fish relative to the controls (Figure 9D; Excel Table S2). Comparison of DEGs from 3 and 7 dpf revealed 4 of the 10 genes to be common to both the time points. Among these, 3 were down-regulated and 1 was up-regulated, with only 2 being annotated. Two of the 3 shared down-regulated genes were neurofilament genes required for maintaining axonal integrity (*nefmb* and *neflb*) (reviewed by Julien and Mushynski 1998; Yuan et al. 2012) (Excel Table S2).

Discussion

Early development is a period of enhanced sensitivity to effects of DomA exposure and low doses of DomA can lead to persistent behavioral deficits, as shown in rodent models (Burt et al. 2008a; Doucette et al. 2004; Levin et al. 2005, 2006; Shiotani et al. 2017; Tanemura et al. 2009; Tryphonas et al. 1990; Xi et al. 1997). However, the mechanisms that underlie these changes are largely

unknown. This study in zebrafish identified the period around 2 dpf as a window of susceptibility to DomA neurodevelopmental toxicity and then characterized the resulting molecular, structural, and behavioral consequences of exposures during this period. Exposure to DomA during this window led to changes in gene expression, disruption of myelin sheath formation in the spinal cord, and aberrant startle behavior.

Use of a Novel Exposure Method to Assess the Window of Susceptibility to Low Doses of DomA

This study established zebrafish as a model for investigating the mechanisms of toxicity from low-dose exposures to DomA during development. Previous developmental DomA exposure studies in zebrafish were done by injecting DomA into the yolk during the early embryonic stages (512–1,000 cell stage) (Tiedeken et al. 2005; Tiedeken and Ramsdell 2007). However, the DomA doses that led to behavioral phenotypes were also those that resulted in

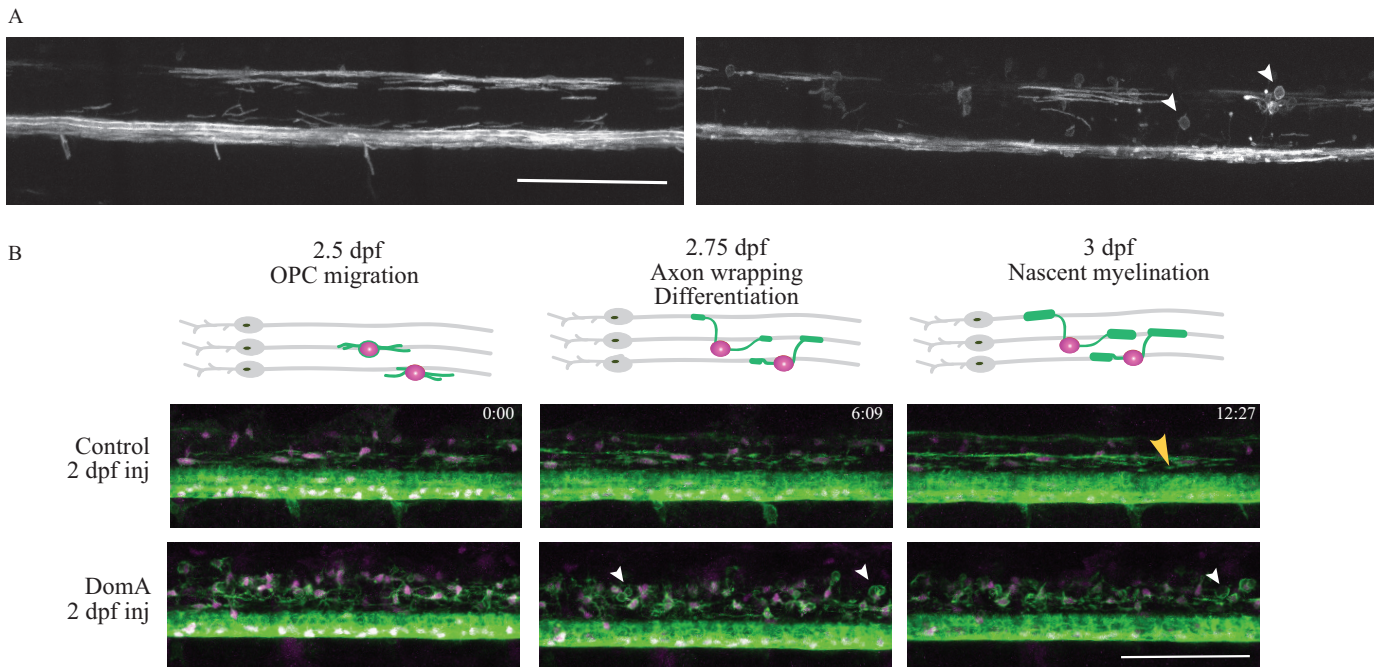


Figure 8. Time-lapse imaging of myelin sheath formation in zebrafish exposed to domoic acid (DomA) at 2 d postfertilization (dpf). (A) *Tg(mbp:EGFP-CAAX)* fish were used to visualize labeled myelin sheaths. Shown are representative images of DomA-exposed (0.14 ng) (right panel), and control larvae (left panel) that were exposed at 2 dpf and imaged at 3 dpf. White arrowheads denote the aberrant circular protrusions found in DomA-exposed larvae (control, $n = 5$; DomA, $n = 10$). (B) Stills from time-lapse imaging of a representative control and DomA-exposed transgenic fish [*Tg(nkx2.2:mEGFP) × Tg(sox10:RFP)*] from 2.5–3 dpf. Time stamps (hour:minutes) show the time elapsed. Diagrams above the images show the key developmental processes in the oligodendrocyte lineage during this time range (representative time-lapse image of control, $n = 5$ and DomA, $n = 6$). Large yellow arrowhead denotes an elongated myelin sheath. Small white arrowheads denote unusual circular myelin membranes. Scale bar: 100 μm . Stills (B) were from a time lapse of control (Video S2) and DomA-exposed fish (Video S3).

high mortality rates and lasting neurotoxic symptoms. To build on this work, we used a novel exposure method in which DomA was delivered intravenously at different periods in development—from the embryonic to the larval stages at doses 3- to 260-fold lower than previously used in zebrafish.

Using this method, we identified the period around 2 dpf as a window of susceptibility for low doses of DomA (nominal doses 0.09–0.14 ng/embryo) at which structural and behavioral effects occurred with no appreciable mortality and minimal gross morphological defects.

Role of Dose and Timing of DomA Exposure on Startle Responses

In zebrafish, the window of susceptibility was identified as 2 dpf; exposure during this period led to persistent behavioral deficits even at the lowest dose of DomA tested (0.09 ng). Although exposure at both 1 and 2 dpf led to acute, nonlethal neurotoxic phenotypes in embryos, they were transient, declining significantly 1 d after exposure and absent by 5 dpf (Figure S3). In contrast, behavioral deficits in startle persisted into later larval stages (7 dpf). Only fish exposed at 2 dpf showed startle deficits at the lowest dose tested (0.09 ng) for all metrics assessed: responsiveness, bend angle, and Mav. In comparison, fish exposed to DomA at 1 dpf had startle deficits only when exposed to higher doses of DomA (0.14–0.18 ng) (Figures 2–4). Furthermore, even when exposed to the higher doses of DomA, fish exposed at 1 dpf had less pronounced kinematic deficits than those exposed at 2 dpf (Figure S4). All this evidence suggests that whereas exposures at different times during early embryonic development can lead to acute, transient effects, there is a critical period around 2 dpf of enhanced sensitivity to these more persistent behavioral deficits. Exposure prior to this period (i.e., at 1 dpf) was associated with both reduced toxin potency and reduced severity of

effects, potentially because DomA was present at lower concentrations during the critical window at 2 dpf. In comparison, 4 dpf is a period after this defined window, and as a result only a subset of fish exposed to the highest doses (0.18 ng) had behavior deficits, which were observed only inconsistently among multiple trials and occurred in conjunction with overt neurotoxic phenotypes (opaque brains described in Table S3).

Role of Dose and Timing of DomA Exposure on Myelin Formation

As seen for the behavioral results, 2 dpf was also a window of susceptibility for disruption of myelin; fish exposed to DomA at 2 dpf showed myelin defects in the spinal cord, even at the lowest doses tested (Figures 5–7). By exposing embryos to DomA at other developmental time points around 2 dpf (1, 2.5, 3 dpf), we were able to more precisely identify the window of susceptibility. We found that fish exhibited less severe and less prevalent myelin defects the further the exposure occurred from the 2 dpf developmental period (Figure 6). One exception was the appearance of a distinct myelin phenotype (Category 5) in a subset of fish exposed at 3 dpf (Figure 6). The uneven, sloughed appearance of myelin in these fish suggests a phenotype that may involve mechanisms distinct from those proposed below. Both the structural phenotype and the mechanisms that underlie these would need to be addressed in future studies.

Fish exposed to DomA at 2 dpf had an overall reduction in labeled myelin, along with the appearance of unusual circular membranes (Figures 5B and 6A). These deficits were visible as early as 3 dpf, when nascent myelin sheaths are present (Figure 8A), and persisted until at least 7 dpf (Figure 7B). Furthermore, time-lapse data showed that even the initial stages of axon wrapping and nascent sheath formation at 2.5 dpf were perturbed (Figure 8B). All this suggests that when DomA exposure closely

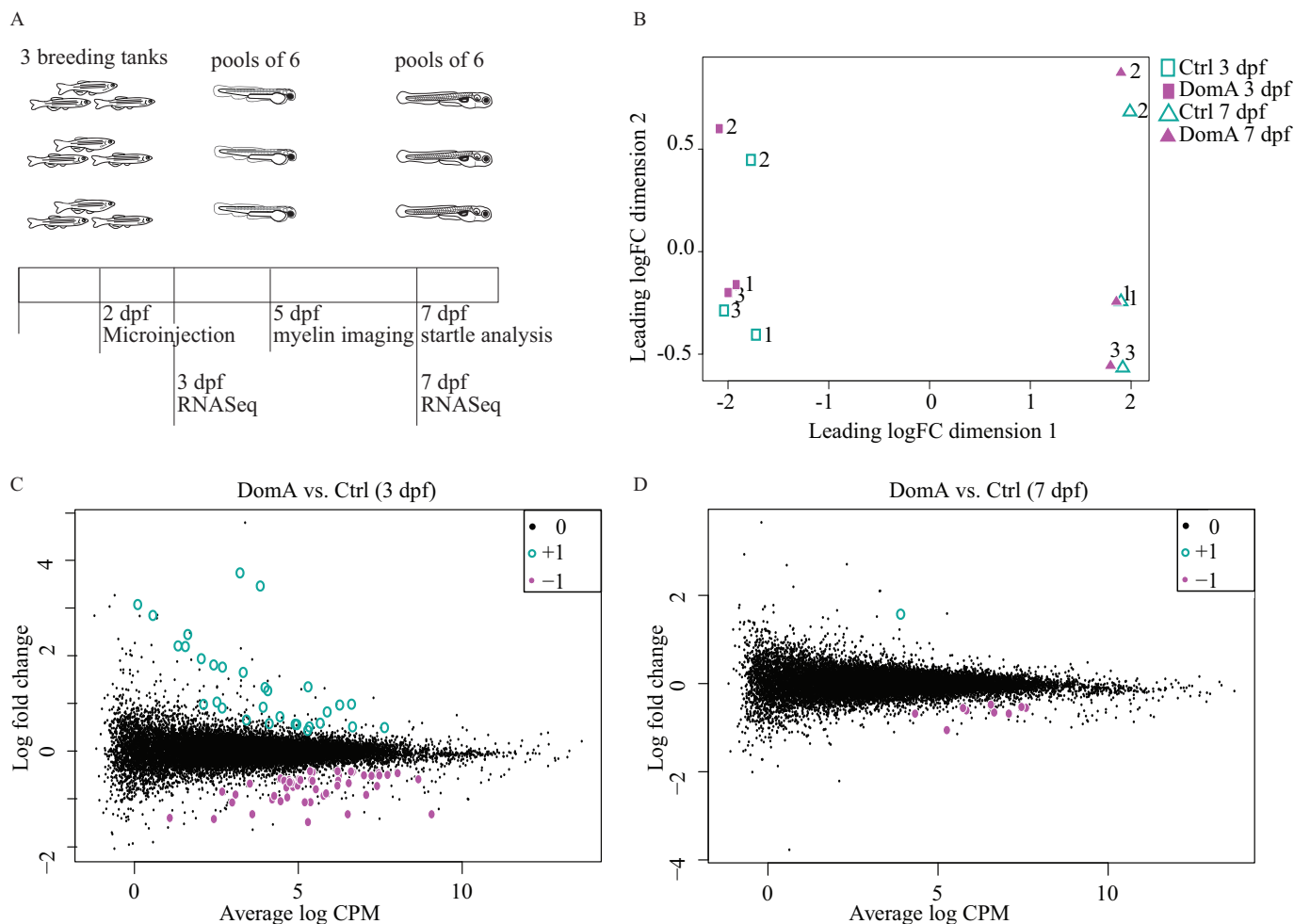


Figure 9. Transcriptional changes associated with domoic acid (DomA) exposure at 2 d postfertilization (dpf). (A) Experimental design. Tanks of three adult fish (2 females, 1 male) of *Tg(mbp:EGFP-CAAX)* background were bred and the embryos exposed to DomA (0.14 ng) or vehicle at 2 dpf. Pools of six embryos within a given treatment from each tank were then sampled at 3 and 7 dpf for RNA sequencing. Three pools per treatment represented the three biological replicates. For functional analyses, myelin sheath labeling was assessed at 5 dpf and startle response was assessed at 7 dpf prior to RNA sequencing. The results confirming differences in behavior and myelin labeling between DomA-exposed fish and controls used for RNA sequencing are shown in Figure S6. (B) A multidimensional scaling plot shows clustering of samples based on overall differences in expression profiles. (C,D) Mean-difference plots compare the log fold changes of genes in DomA-exposed vs. control fish at the 3 dpf- and 7 dpf-sampling times. Hollow teal circles (+1) represent genes that were significantly up-regulated in DomA-exposed fish relative to their controls, whereas filled magenta circles (-1) represent genes that were significantly down-regulated in DomA-exposed fish relative to their controls. Significance was determined with a gene-wise negative binomial generalized linear model with a quasi-likelihood test. *p*-Values were adjusted for using a 5% false discovery rate cutoff. Tables S30 and S31 contain the results of the functional enrichment analysis done using the differentially expressed genes shown in (C). Excel Table S1 contains the list of genes that were differentially expressed in DomA-exposed fish at 3 dpf, and Excel Table S2 contains the list of genes that were differentially expressed in DomA-exposed fish at 7 dpf. Note: CPM, counts per million; FC, fold change.

precedes the formation of myelin (exposures at 2 dpf), it disrupts the initial formation of myelin, leading to lasting myelin defects that do not recover within 5 d postexposure. Consistent with this, we saw very few myelin defects when DomA exposure occurred at 4 dpf—a time point after nascent myelin has been established. The absence of a myelin phenotype following exposure at 4 dpf suggests that DomA, at least at the low to intermediate doses used here, may not disrupt already established sheaths but, rather, may perturb the initial formation of myelin sheaths.

Comparison of the Window of Susceptibility to DomA Corresponds to Critical Periods in Oligodendrocyte Development

The 2-dpf window of susceptibility suggests that DomA may perturb specific developmental processes that occur within this time period. Although most of the early neurons have already differentiated by 2 dpf, the oligodendrocyte lineage—the lineage that

myelinates axons in the central nervous system—is just beginning to migrate and differentiate during this period (Brösamle and Halpern 2002; Kirby et al. 2006). DomA exposure at 2 dpf may perturb critical processes in oligodendrocyte development, leading to the observed disrupted myelination.

Both myelinating oligodendrocytes and their precursors express functional ionotropic glutamate receptors, making them potential cellular targets for DomA (Kolodziejczyk et al. 2010; Patneau et al. 1994). KA, a structural analog of DomA, caused cell death in oligodendrocyte primary cell cultures at concentrations comparable to those affecting neurons (Alberdi et al. 2002; McDonald et al. 1998; Sánchez-Gómez and Matute 1999). Binding to and activating glutamate receptors through the application of AMPA or KA inhibited proliferation and lineage progression in oligodendrocyte progenitor cells (Gallo et al. 1996). Mature oligodendrocytes exhibited demyelination after chronic direct infusion of KA on the optic nerves. All of this suggests that DomA may alter oligodendrocyte development and that

exposure to DomA at 2 dpf may disrupt critical processes important for OPC survival, proliferation, or myelin sheath formation.

Our results showing myelin defects after DomA exposure are consistent with those of a previous study in which 11-wk-old juvenile mice exposed to DomA *in utero* during gestational days 11.5 and 14.5, but not 17.5, had less staining for the myelin-associated glycoprotein in their cerebral cortices (Tanemura et al. 2009). Our findings extend this work by identifying altered myelination in the spinal cord and revealing that DomA does not disrupt already established myelin sheaths but, rather, perturbs the initial formation of the sheaths during a specific window in development. It is possible that sensitivity at the early periods is due to disruptions in oligodendrocyte development, thereby altering their ability to form myelin sheaths during the postnatal period (Foran and Peterson 1992; Verity and Campagnoni 1988).

Influence of Extrinsic Factors on a Critical Window for DomA Toxicity

In addition to the intrinsic sensitivity of developing oligodendrocytes, the 2-dpf window of susceptibility may also be influenced by extrinsic factors that affect the distribution and availability of DomA to the cells and tissues of interest. One process that may influence DomA availability in the central nervous system is the development of the blood–spinal cord barrier (BSCB) and the blood–brain barrier (BBB)—structures that separate the blood from the spinal cord and brain parenchyma, respectively (Bartanusz et al. 2011; Eliceiri et al. 2011), and prevent the diffusion of water-soluble molecules (Fleming et al. 2013; Jeong et al. 2008; Xie et al. 2010). In zebrafish, the BBB forms between 3 and 10 dpf, and thus DomA may be increasingly excluded from the brain after 2 dpf. Although less is known about the formation of the BSCB, dye exclusion experiments suggest it may form later in development, excluding high-molecular weight compounds (fluorescein isothiocyanate dextran, 2,000 kDa) at 3 dpf

(Jeong et al. 2008), and smaller molecular weight ones (961 Da) by 8 dpf (Fleming et al. 2013).

DomA may also be less accessible to cell targets later in development due to higher excretion rates as the kidney matures. In mammals, DomA is primarily cleared from the plasma via the kidneys (Lefebvre et al. 2007; Preston and Hynie 1991; Suzuki and Hierlihy 1993). In zebrafish, glomerular filtration begins at around 2 dpf, whereas full maturation of the kidney occurs by 4 dpf (Drummond and Davidson 2010; Drummond 2005). Thus, DomA may be more readily cleared during periods in development after 2 dpf.

DomA-Induced Transcriptional Changes

RNA-seq analysis identified genes and pathways that were consistent with the imaging and behavioral data. DomA exposure down-regulated genes required for maintaining myelin structure, including myelin protein zero (*mpz*) and myelin basic protein a (*mbpa*), along with genes required for maintaining axonal structure (*nefla*, *neflb*, *nefma*, *nefmb*) (Figure 10). Stathmin genes were also over-represented. Stathmins destabilize microtubules by sequestering free tubulin and play critical roles in modulating neurite outgrowth and branching in the developing nervous system (Grenningloh et al. 2004; Wen et al. 2010). It has also been shown that the dysregulation of different stathmin genes (either through down- or up-regulation) can lead to alterations in microtubule density and axonal integrity (Cheng et al. 1997; Wen et al. 2010, 2013).

The altered expression of axonal structural genes suggests that possibility that DomA may be primarily targeting axons and that the myelination defects may be a secondary effect. AMPA receptors are widely expressed in neurons and neuronal precursors in the brain and spinal cord of developing zebrafish (Hoppmann et al. 2008). Alternatively, DomA may perturb oligodendrocyte development and myelin wrapping, leading to later axonal dysfunction. Further work is underway to investigate the potential axonal targets of DomA toxicity and to assess the

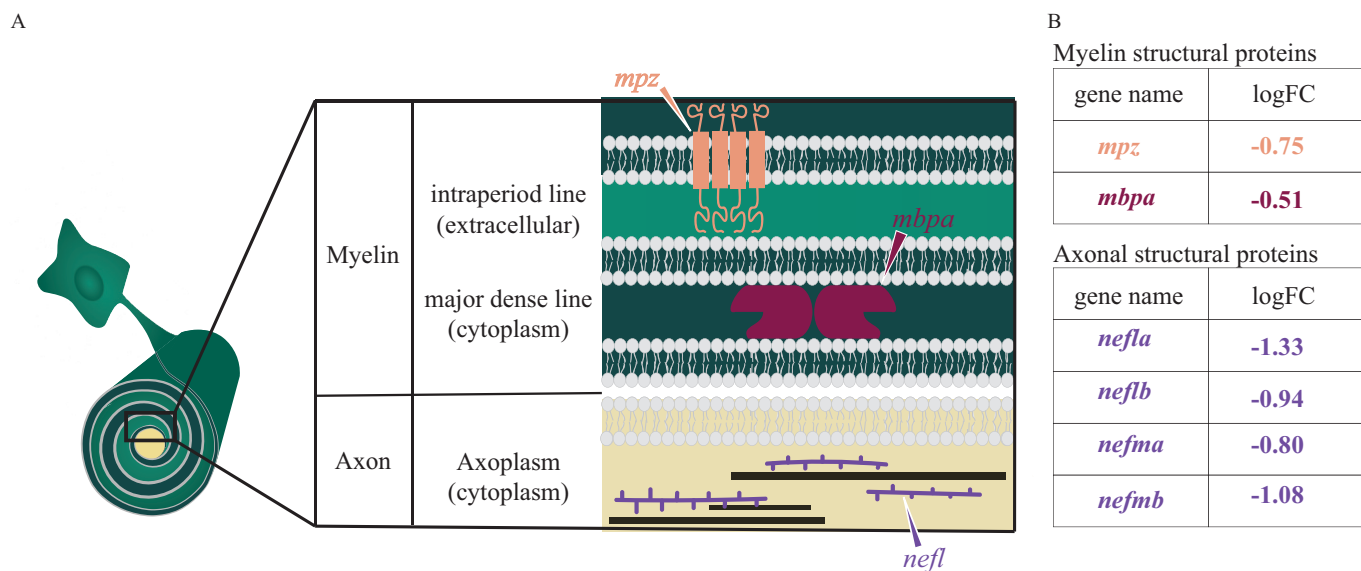


Figure 10. Diagram of myelin and axonal structural proteins differentially expressed in domoic acid (DomA)-exposed fish. (A) Schematic of the cross section of an axon–myelin interface with a focus on selected myelin and axon structural proteins that are differentially expressed in DomA-exposed fish at 3 d postfertilization. The magnified cross section shows the major divisions in myelin (Barkovich 2000): first, major dense line: the electron-dense cytoplasm where myelin basic protein (encoded by the *mbp* gene) attaches to the inner surface of the membrane proteins and stabilizes myelin, and second, the intraperiod line, the less electron-dense extracellular space. Transmembrane proteins like myelin protein zero (encoded by the *mpz* gene) maintains compact myelin structure through its cytoplasmic and extracellular interactions. The cross section also shows a simplified axoplasm that contains neurofilaments that form part of the axon cytoskeleton. (B) Myelin and structural proteins that are differentially expressed, with their log fold change (logFC). –, gene was down-regulated in DomA-exposed fish relative to controls.

contribution of the axonal disruptions to the myelin sheath phenotypes that we characterized here (Panlilio 2019).

RNA-seq data showed higher expression of glial fibrillary acidic protein (*gfap*) in DomA-exposed fish relative to controls. The up-regulation of *gfap* in mammals is a hallmark of reactive astrogliosis—the response of astrocytes following mechanical injury, excitotoxicity, and ischemia (Brenner 2014; Burtrum and Silverstein 1993; Eng and Ghimikar 1994; Pekny and Nilsson 2005). In contrast, zebrafish and other teleosts have *gfap*-expressing cells that include radial glial cells previously thought to functionally substitute for astrocytes (Baumgart et al. 2012; Lyons and Talbot 2015). Zebrafish may have a subpopulation of *gfap*⁺ cells that have characteristics similar to those of mammalian astrocytes, but it is yet to be determined whether these newly described astrocytes respond to injury (Chen et al. 2020). Although the cells that express *gfap* include cell types other than astrocytes, the overall response is similar: *gfap* expression is higher near the site of large injuries that result from brain stabs (Baumgart et al. 2012; März et al. 2011), spinal cord transections (Hui et al. 2010; Mokalled et al. 2016), and excitotoxic lesions (Skaggs et al. 2014). In contrast to mammals, fish have robust regenerative mechanisms, and the up-regulation of *gfap* and the infiltration of ependymoglia results in tissue repair and functional integration rather than scar formation that occurs in mammals (Adams and Gallo 2018; Baumgart et al. 2012; Hui et al. 2015; März et al. 2011). Notably, these studies have been done in adult fish, and *gfap* up-regulation occurs over multiple days after injury, so it may be difficult to generalize these findings to studies with injuries that occur in early development. Nonetheless, the up-regulation of *gfap* at 3 dpf following exposure to DomA at 2 dpf suggests that DomA exposure may have both led to injury and triggered repair mechanisms associated with higher *gfap* expression.

We did not validate our RNA-seq results with qPCR. There is no clear consensus on whether it is necessary to validate RNA-seq data using qRT-PCR (Fang and Cui 2011). Here, RNA-seq was used as an initial exploratory tool to identify potential cellular processes and structures perturbed by DomA. RNA-seq analyses will need to be followed up using more targeted approaches.

Implications for Human Health

Timing and targets. This study provides a careful examination of potential windows of susceptibility to DomA exposure. The identification of key processes disrupted during these windows of susceptibility has important implications for identifying hazards for early developmental exposures in humans. Unlike in zebrafish, myelination in humans occurs over a prolonged period, starting *in utero* and continuing into early childhood and adolescence. The progression of myelination is mostly conserved across species, with myelination commencing in the periphery, brainstem, and spinal cord, then progressing rostrally to the forebrain (Rice and Barone 2000; Tanaka et al. 1995). The most widespread and rapid period of myelination in humans occurs within the first 2 years of infancy (Kinney et al. 1988; Kinney and Volpe 2018). Although most of the major tracts are myelinated by 3–5 years of age, myelination is now known to continue into adulthood, especially in cortical regions where changes in myelination are associated with experience and learning new skills (Fields 2005; Pajevic et al. 2014). Thus, for humans, there may not be a single window of susceptibility but, rather, multiple windows; DomA may perturb myelin formation in specific regions of the nervous system in which myelination coincides with the timing of exposures.

In this study, we showed that myelination was perturbed in the spinal cord. Despite evidence that acute exposure to DomA in humans can lead to the degeneration of neurons within the spinal

cord (Teitelbaum et al. 1990), there has been little research on the spinal cord as a target tissue for DomA toxicity. Only one other study in rodents has investigated the spinal cord as a target tissue for DomA exposures. Wang et al. (2000) found that postnatal exposures to high doses of DomA led to spinal cord lesions by 2 h postexposure, even in the absence of any histological damage to selected brain regions, including the well-known target, the hippocampus (Wang et al. 2000). Our study confirms the spinal cord as a potential target and identifies myelination as a process perturbed in the spinal cord.

Behavioral analogies. We used startle response behavior as a functional readout of neurodevelopmental toxicity. Deficits in the kinematics of startle responses are reminiscent of motor deficits found in incidental human exposures, chronic exposures in primates, and developmental exposures in rodents. Adult humans acutely exposed to DomA developed sensorimotor neuropathy and axonopathy as assessed by electromyography (Teitelbaum et al. 1990). A subset of the primates exposed orally at or near the accepted daily tolerable dose of 0.075 mg/kg developed visible hand tremors (Petroff et al. 2019). Rodents prenatally exposed to DomA [postnatal days (PND) 10–17] developed aberrant gait patterns including impaired interlimb coordination and aberrant step sequence patterns (Shiotani et al. 2017).

Although there is evidence that DomA can perturb motor function, developmental exposures to DomA in rodents have not led to reductions in startle response amplitude during baseline conditions (prior to habituation or pre-pulse inhibition tests) (Adams et al. 2008; Marriott et al. 2012; Shiotani et al. 2017; Zuloaga et al. 2016). This may be because exposures to DomA in these rodent models were done during a period that does not correspond to development of the startle circuit. Furthermore, there are some notable differences between rodent and fish startle, including distinct baseline startle kinematics and variations in the specific neuronal subsets in the circuits (Eaton et al. 2001; Koch 1999; Yeomans and Frankland 1995). Despite these differences, measuring startle response behavior in fish provides a tool to assess sensory processing and motor control and how these processes are perturbed by toxin exposure.

Doses and toxicokinetics. In previous experimental studies involving developmental exposure to DomA, low doses have been defined based on the absence of acute neurotoxic symptoms, rather than by a specific dose. Low doses are those that do not lead to classic acute symptoms that include tremors, scratching, and convulsions either in mothers (prenatal exposures) or in the pups directly exposed to DomA (postnatal exposures). Our study used nominal doses that were 3- to 260-fold lower than those used previously in zebrafish; these lower doses caused only transient acute effects in embryos but led to persistent behavioral effects and myelin defects. The weight-normalized doses (dosages) of DomA used in our zebrafish experiments are comparable to those used in the majority of the postnatal rodent studies (Adams et al. 2008; Bernard et al. 2007; Doucette et al. 2004; Gill et al. 2010; Marriott et al. 2012; Perry et al. 2009; Tasker et al. 2005). Assuming a 1.4-mg wet weight per embryo (Tiedeken et al. 2005), the dosages at which zebrafish embryos consistently exhibited myelin defects and behavioral deficits in our experiments were 0.06–0.10 mg/kg DomA. In comparison, rodents that showed behavioral deficits following postnatal exposure were dosed subcutaneously with seven injections of 0.005 and 0.020 mg/kg DomA between PND 8–14, leading to similar cumulative DomA dosages of 0.035–0.14 mg/kg.

Challenges associated with translating doses used in animal studies to humans include the dearth of human exposure and toxicokinetic data, species differences in sensitivity to DomA, and differences in bioavailability for different routes of exposure

(reviewed by [Costa et al. 2010](#); [Lefebvre and Robertson 2010](#)). There is currently no information on DomA concentrations in human fetal tissues or fluids, or even in maternal plasma. Human exposures to DomA are only estimated from consumption data, average weights of adults, and measured DomA concentrations in shellfish. From such data it is estimated that adults exhibiting acute neurotoxicity in a 1987 incident consumed approximately 1–5 mg DomA/kg body weight ([Wekell et al. 1994](#)). Tolerable oral daily intake (TDI) values of 0.075–0.100 mg/kg per day have been calculated from nonhuman primate and human data, also for acute neurotoxic effects ([Costa et al. 2010](#); [Mariën 1996](#)). However, chronic exposure of pregnant monkeys at or near the TDI (0.075 and 0.150 mg/kg) led to impaired memory in offspring ([Grant et al. 2019](#)). The toxicokinetic behavior of consumed DomA in humans is not known. However, research in nonhuman primates showed that oral exposures to DomA led to extended half-lives (almost 10× the length of the half-life following intravenous exposures) ([Jing et al. 2018](#)).

Even less information exists about the elimination and distribution in DomA in fetuses when mothers are exposed to DomA. One study in rodents showed that at 1 h following intravenous injection of Dom A at GD13, concentrations of DomA found in fetal brains, amniotic fluid, and maternal brains were similar ([Maucher and Ramsdell 2007](#)). This suggests that earlier in development there are no barriers for DomA entry to the fetal brain and that DomA in the fetal brain reaches equilibrium concentrations with DomA in the amniotic fluid. Emerging evidence from marine mammals shows that DomA can remain in the fetal fluids (amniotic and allantoic fluids) over prolonged periods of time ([Brodie et al. 2006](#); [Lefebvre et al. 2018](#)). Thus, DomA may be recirculated within the fetal fluid compartments, allowing for continuous exposures in fetuses, even when maternal plasma has reached undetectable levels of DomA. Recent studies in nonhuman primates also show recirculation of DomA between fetus and amniotic fluid, leading to a longer apparent fetal half-life than the maternal half-life ([Shum et al. 2020](#)). Ultimately, data on human fetal exposure levels will be needed to more fully understand the implications of results from animal models.

Conclusions

DomA is a well-known developmental neurotoxin. However, few studies have been able to identify the cellular and molecular processes that underlie the observed behavioral deficits seen following developmental exposures. Using zebrafish, we were able to deliver DomA at specific developmental times and link behavioral deficits to structural changes in the neural circuit required for the behavior. The results from this study show that there is a critical window of susceptibility to DomA and that exposure leads to altered expression of key axonal and myelin structural genes, disruptions to myelination, and later perturbations to startle behavior. These results establish the zebrafish as a model for investigating the cellular and molecular mechanisms underlying DomA-induced developmental neurotoxicity.

Acknowledgments

We thank H.E. Rivera and A.R. Solow for their advice on the statistical analysis, H. Burgess for providing the Flote software for startle kinematic analysis, I.T. Jones for measuring the vibrational output of the startle setup, B.G. Merrick for his help designing and building the startle apparatus, and L. Kerr for microscopy training and advice (MBL microscopy facility). We also thank the labs who generously provided us with zebrafish transgenic lines to make this work possible: B. Appel (University of Colorado, Denver), S. Kucenas (University of Virginia), and

D. Lyons (University of Edinburg). In addition, we thank four anonymous reviewers and the *EHP* Science Editor for helpful suggestions on an earlier version of the manuscript.

This research was supported by the Oceans Venture Fund, the Von Damm Fellowship, the Ocean Ridge Initiative Fellowship, and Woods Hole Sea grant (NA14OAR4170074) (all to J.M.P.), and by the Woods Hole Center for Oceans and Human Health (NIH: P01ES021923 and P01ES028938; NSF: OCE-1314642 and OCE-1840381; Center PI: John Stegeman, Project PI: M.E.H.).

References

- Adams AL, Doucette TA, Ryan CL. 2008. Altered pre-pulse inhibition in adult rats treated neonatally with domoic acid. *Amino Acids* 35(1):157–160, PMID: [17973071](#), <https://doi.org/10.1007/s00726-007-0603-3>.
- Adams KL, Gallo V. 2018. The diversity and disparity of the glial scar. *Nat Neurosci* 21(1):9–15, PMID: [29269757](#), <https://doi.org/10.1038/s41593-017-0033-9>.
- Alberdi E, Sánchez-Gómez MV, Marino A, Matute C. 2002. Ca²⁺ influx through AMPA or kainate receptors alone is sufficient to initiate excitotoxicity in cultured oligodendrocytes. *Neurobiol Dis* 9(2):234–243, PMID: [11895374](#), <https://doi.org/10.1006/nbdi.2001.0457>.
- Almeida RG, Czopka T, Ffrench-Constant C, Lyons DA. 2011. Individual axons regulate the myelinating potential of single oligodendrocytes in vivo. *Development* 138(20):4443–4450, PMID: [21880787](#), <https://doi.org/10.1242/dev.071001>.
- Anders S, Pyl PT, Huber W. 2015. HTSeq—a Python framework to work with high-throughput sequencing data. *Bioinformatics* 31(2):166–169, PMID: [25260700](#), <https://doi.org/10.1093/bioinformatics/btu638>.
- Andrews S. 2010. FastQC: a quality control tool for high throughput sequence data. <http://www.bioinformatics.babraham.ac.uk/projects/fastqc/> [accessed 7 October 2020].
- Arrenberg AB, Driever W. 2013. Integrating anatomy and function for zebrafish circuit analysis. *Front Neural Circuits* 7(74), PMID: [23630469](#), <https://doi.org/10.3389/fncir.2013.00074>.
- Barkovich AJ. 2000. Concepts of myelin and myelination in neuroradiology. *AJNR Am J Neuroradiol* 21(6):1099–1109, PMID: [10871022](#).
- Bartanusz V, Jezova D, Alajajian B, Digicaylioglu M. 2011. The blood–spinal cord barrier: morphology and clinical implications. *Ann Neurol* 70(2):194–206, PMID: [21674586](#), <https://doi.org/10.1002/ana.22421>.
- Bates D, Mächler M, Bolker B, Walker S. 2015. Fitting linear mixed-effects models using lme4. *J Stat Softw* 67(1):1–48, <https://doi.org/10.18637/jss.v067.i01>.
- Baumgart EV, Barbosa JS, Bally-Cuif L, Götz M, Ninkovic J. 2012. Stab wound injury of the zebrafish telencephalon: a model for comparative analysis of reactive gliosis. *Glia* 60(3):343–357, PMID: [22105794](#), <https://doi.org/10.1002/glia.22269>.
- Benaglia T, Chauveau D, Hunter DR, Young DS. 2009. mixtools: an R package for analyzing mixture models. *J Stat Softw* 32(6):1–29, <https://doi.org/10.18637/jss.v032.i06>.
- Benjamini Y, Hochberg Y. 1995. Controlling the false discovery rate: a practical and powerful approach to multiple testing. *J R Stat Soc Series B Stat Methodol* 57(1):289–300.
- Bernard PB, MacDonald DS, Gill DA, Ryan CL, Tasker RA. 2007. Hippocampal mossy fiber sprouting and elevated trkB receptor expression following systemic administration of low dose domoic acid during neonatal development. *Hippocampus* 17(11):1121–1133, PMID: [17636548](#), <https://doi.org/10.1002/hipo.20342>.
- Boggs JM. 2006. Myelin basic protein: a multifunctional protein. *Cell Mol Life Sci* 63(17):1945–1961, PMID: [16794783](#), <https://doi.org/10.1007/s00018-006-6094-7>.
- Bolger AM, Lohse M, Usadel B. 2014. Trimmomatic: a flexible trimmer for Illumina sequence data. *Bioinformatics* 30(15):2114–2120, PMID: [24695404](#), <https://doi.org/10.1093/bioinformatics/btu170>.
- Brenner M. 2014. Role of GFAP in CNS injuries. *Neurosci Lett* 565:7–13, PMID: [24508671](#), <https://doi.org/10.1016/j.neulet.2014.01.055>.
- Brodie EC, Gulland FMD, Greig DJ, Hunter M, Jaakola J, St. Leger J, et al. 2006. Domoic acid causes reproductive failure in California sea lions (*Zalophus californianus*). *Mar Mamm Sci* 22(3):700–707, <https://doi.org/10.1111/j.1748-7692.2006.00045.x>.
- Brösamle C, Halpern ME. 2002. Characterization of myelination in the developing zebrafish. *Glia* 39(1):47–57, PMID: [12112375](#), <https://doi.org/10.1002/glia.10088>.
- Burgess HA, Granato M. 2007. Modulation of locomotor activity in larval zebrafish during light adaptation. *J Exp Biol* 210(pt 14):2526–2539, PMID: [17601957](#), <https://doi.org/10.1242/jeb.003939>.
- Burtrum D, Silverstein FS. 1993. Excitotoxic injury stimulates glial fibrillary acidic protein mRNA expression in perinatal rat brain. *Exp Neurol* 121(1):127–132, PMID: [8495707](#), <https://doi.org/10.1006/exnr.1993.1078>.

- Burt MA, Ryan CL, Doucette TA. 2008a. Altered responses to novelty and drug reinforcement in adult rats treated neonatally with domoic acid. *Physiol Behav* 93(1–2):327–336, PMID: 17980392, <https://doi.org/10.1016/j.physbeh.2007.09.003>.
- Burt MA, Ryan CL, Doucette TA. 2008b. Low dose domoic acid in neonatal rats abolishes nicotine induced conditioned place preference during late adolescence. *Amino Acids* 35(1):247–249, PMID: 17701097, <https://doi.org/10.1007/s00726-007-0584-2>.
- Chen J, Poskanzer KE, Freeman MR, Monk KR. 2020. Live-imaging of astrocyte morphogenesis and function in zebrafish neural circuits. *Nat Neurosci* 23(10):1297–1306, PMID: 32895565, <https://doi.org/10.1038/s41593-020-0703-x>.
- Chen Y, Lun ATL, Smyth GK. 2016. From reads to genes to pathways: differential expression analysis of RNA-Seq experiments using Rsubread and the edgeR quasi-likelihood pipeline. *F1000Res* 5:1438, PMID: 27508061, <https://doi.org/10.12688/f1000research.8987.2>.
- Cheng HW, Jiang T, Mori N, McNeill TH. 1997. Upregulation of stathmin (p19) gene expression in adult rat brain during injury-induced synapse formation. *Neuroreport* 8(17):3691–3695, PMID: 9427352, <https://doi.org/10.1097/00001756-199712010-00007>.
- Cianciolo Cosentino C, Roman BL, Drummond IA, Hukriede NA. 2010. Intravenous microinjections of zebrafish larvae to study acute kidney injury. *J Vis Exp* 42:2079, PMID: 20729805, <https://doi.org/10.3791/2079>.
- Costa LG, Giordano G, Faustman EM. 2010. Domoic acid as a developmental neurotoxin. *Neurotoxicology* 31(5):409–423, PMID: 20471419, <https://doi.org/10.1016/j.neuro.2010.05.003>.
- Czopka T. 2016. Insights into mechanisms of central nervous system myelination using zebrafish. *Glia* 64(3):333–349, PMID: 26250418, <https://doi.org/10.1002/glia.22897>.
- Dobin A, Davis CA, Schlesinger F, Drenkow J, Zaleski C, Jha S, et al. 2013. STAR: ultrafast universal RNA-seq aligner. *Bioinformatics* 29(1):15–21, PMID: 23104886, <https://doi.org/10.1093/bioinformatics/bts635>.
- Doucette TA, Bernard PB, Husum H, Perry MA, Ryan CL, Tasker RA. 2004. Low doses of domoic acid during postnatal development produce permanent changes in rat behaviour and hippocampal morphology. *Neurotox Res* 6(7–8):555–563, PMID: 15639787, <https://doi.org/10.1007/BF03033451>.
- Drummond IA. 2005. Kidney development and disease in the zebrafish. *J Am Soc Nephrol* 16(2):299–304, PMID: 15647335, <https://doi.org/10.1681/ASN.2004090754>.
- Drummond IA, Davidson AJ. 2010. Zebrafish kidney development. *Methods Cell Biol* 100:233–260, PMID: 21111220, <https://doi.org/10.1016/B978-0-12-384892-5.00009-8>.
- Eaton RC, Lee RKK, Foreman MB. 2001. The Mauthner cell and other identified neurons of the brainstem escape network of fish. *Prog Neurobiol* 63(4):467–485, PMID: 11163687, [https://doi.org/10.1016/S0301-0082\(00\)00047-2](https://doi.org/10.1016/S0301-0082(00)00047-2).
- Eliceiri BP, Gonzalez AM, Baird A. 2011. Zebrafish model of the blood-brain barrier: morphological and permeability studies. *Methods Mol Biol* 686:371–378, PMID: 21082382, https://doi.org/10.1007/978-1-60761-938-3_18.
- Eng LF, Ghirmikar RS. 1994. GFAP and astroglia. *Brain Pathol* 4(3):229–237, PMID: 7952264, <https://doi.org/10.1111/j.1750-3639.1994.tb00838.x>.
- Fang Z, Cui X. 2011. Design and validation issues in RNA-seq experiments. *Brief Bioinform* 12(3):280–287, PMID: 21498551, <https://doi.org/10.1093/bib/bbr004>.
- Fetcho JR, Higashijima S-I. 2004. Optical and genetic approaches toward understanding neuronal circuits in zebrafish. *Integr Comp Biol* 44(1):57–70, PMID: 21680486, <https://doi.org/10.1093/icb/44.1.57>.
- Fields RD. 2005. Myelination: an overlooked mechanism of synaptic plasticity? *Neuroscientist* 11(6):528–531, PMID: 16282593, <https://doi.org/10.1177/1073858405282304>.
- Fleming A, Diekmann H, Goldsmith P. 2013. Functional characterisation of the maturation of the blood-brain barrier in larval zebrafish. *PLoS One* 8(10):e77548, PMID: 24147021, <https://doi.org/10.1371/journal.pone.0077548>.
- Foran DR, Peterson AC. 1992. Myelin acquisition in the central nervous system of the mouse revealed by an MBP-Lac Z transgene. *J Neurosci* 12(12):4890–4897, PMID: 1281497, <https://doi.org/10.1523/JNEUROSCI.12-12-04890.1992>.
- Fox J, Weisberg S. 2018. *An R Companion to Applied Regression*. 3rd ed. Thousand Oaks, CA: SAGE Publications.
- Gallo V, Zhou JM, McBain CJ, Wright P, Knutson PL, Armstrong RC. 1996. Oligodendrocyte progenitor cell proliferation and lineage progression are regulated by glutamate receptor-mediated K⁺ channel block. *J Neurosci* 16(8):2659–2670, PMID: 8786442, <https://doi.org/10.1523/JNEUROSCI.16-08-02659.1996>.
- Gill DA, Bastlund JF, Watson WP, Ryan CL, Reynolds DS, Tasker RA. 2010. Neonatal exposure to low-dose domoic acid lowers seizure threshold in adult rats. *Neuroscience* 169(4):1789–1799, PMID: 20600646, <https://doi.org/10.1016/j.neuroscience.2010.06.045>.
- Grant KS, Crouthamel B, Kenney C, McKain N, Petroff R, Shum S, et al. 2019. Preclinical modeling of exposure to a global marine bio-contaminant: effects of in utero domoic acid exposure on neonatal behavior and infant memory. *Neurotoxicol Teratol* 73:1–8, PMID: 30690118, <https://doi.org/10.1016/j.ntt.2019.01.003>.
- Grattan LM, Boushey CJ, Liang Y, Lefebvre KA, Castellon LJ, Roberts KA, et al. 2018. Repeated dietary exposure to low levels of domoic acid and problems with everyday memory: research to public health outreach. *Toxins (Basel)* 10(3):103, PMID: 29495583, <https://doi.org/10.3390/toxins10030103>.
- Grattan LM, Boushey C, Tracy K, Trainer VL, Roberts SM, Schluterman N, et al. 2016. The association between razor clam consumption and memory in the CoASTAL Cohort. *Harmful Algae* 57(B):20–25, PMID: 27746706, <https://doi.org/10.1016/j.hal.2016.03.011>.
- Greeningloh G, Soehman S, Bondallaz P, Ruchti E, Cadas H. 2004. Role of the microtubule destabilizing proteins SCG10 and stathmin in neuronal growth. *J Neurobiol* 58(1):60–69, PMID: 14598370, <https://doi.org/10.1002/neu.10279>.
- Guo S. 2004. Linking genes to brain, behavior and neurological diseases: what can we learn from zebrafish? *Genes Brain Behav* 3(2):63–74, PMID: 15005714, <https://doi.org/10.1046/j.1601-183X.2003.00053.x>.
- Hampson DR, Huang XP, Wells JW, Walter JA, Wright JLC. 1992. Interaction of domoic acid and several derivatives with kainic acid and AMPA binding sites in rat brain. *Eur J Pharmacol* 218(1):1–8, PMID: 1383007, [https://doi.org/10.1016/0014-2999\(92\)90140-Y](https://doi.org/10.1016/0014-2999(92)90140-Y).
- Hernandez RE, Galitan L, Cameron J, Goodwin N, Ramakrishnan L. 2018. Delay of initial feeding of zebrafish larvae until 8 days postfertilization has no impact on survival or growth through the juvenile stage. *Zebrafish* 15(5):515–518, PMID: 30089231, <https://doi.org/10.1089/zeb.2018.1579>.
- Higashijima S, Masino MA, Mandel G, Fetcho JR. 2003. Imaging neuronal activity during zebrafish behavior with a genetically encoded calcium indicator. *J Neurophysiol* 90(6):3986–3997, PMID: 12930818, <https://doi.org/10.1152/jn.00576.2003>.
- Højsgaard S, Halekoh U, Yan J. 2006. The R package geepack for generalized estimating equations. *J Stat Softw* 15(2):1–11, <https://doi.org/10.18637/jss.v015.i02>.
- Hoppmann V, Wu JJ, Søviknes AM, Helvik JV, Becker TS. 2008. Expression of the eight AMPA receptor subunit genes in the developing central nervous system and sensory organs of zebrafish. *Dev Dyn* 237(3):788–799, PMID: 18224707, <https://doi.org/10.1002/dvdy.21447>.
- Hothorn T, Bretz F, Westfall P. 2008. Simultaneous inference in general parametric models. *Biom J* 50(3):346–363, PMID: 18481363, <https://doi.org/10.1002/bimj.200810425>.
- Hui SP, Dutta A, Ghosh S. 2010. Cellular response after crush injury in adult zebrafish spinal cord. *Dev Dyn* 239(11):2962–2979, PMID: 20931657, <https://doi.org/10.1002/dvdy.22438>.
- Hui SP, Nag TC, Ghosh S. 2015. Characterization of proliferating neural progenitors after spinal cord injury in adult zebrafish. *PLoS One* 10(12):e0143595, PMID: 26630262, <https://doi.org/10.1371/journal.pone.0143595>.
- Jeffery B, Barlow T, Moizer K, Paul S, Boyle C. 2004. Amnesic shellfish poison. *Food Chem Toxicol* 42(4):545–557, PMID: 15019178, <https://doi.org/10.1016/j.fct.2003.11.010>.
- Jeong J-Y, Kwon H-B, Ahn J-C, Kang D, Kwon S-H, Park JA, et al. 2008. Functional and developmental analysis of the blood-brain barrier in zebrafish. *Brain Res Bull* 75(5):619–628, PMID: 18355638, <https://doi.org/10.1016/j.brainresbull.2007.10.043>.
- Jing J, Petroff R, Shum S, Crouthamel B, Toplez AR, Grant KS, et al. 2018. Toxicokinetics and physiologically based pharmacokinetic modeling of the shellfish toxin domoic acid in nonhuman primates. *Drug Metab Dispos* 46(2):155–165, PMID: 29150543, <https://doi.org/10.1124/dmd.117.078485>.
- Julien JP, Mushynski WE. 1998. Neurofilaments in health and disease. *Prog Nucleic Acid Res Mol Biol* 61:1–23, PMID: 9752717, [https://doi.org/10.1016/S0079-6603\(08\)00823-5](https://doi.org/10.1016/S0079-6603(08)00823-5).
- Kinney HC, Brody BA, Kloman AS, Gilles FH. 1988. Sequence of central nervous system myelination in human infancy. II. Patterns of myelination in autopsied infants. *J Neuropathol Exp Neurol* 47(3):217–234, PMID: 3367155, <https://doi.org/10.1097/00005072-198805000-00003>.
- Kinney HC, Volpe JJ. 2018. Myelination events. In: *Volpe's Neurology of the Newborn*. 6th ed. Volpe JJ, Inder TE, Darras BT, de Vries LS, du Plessis AJ, Neil JJ, et al., eds. Philadelphia, PA: Elsevier, 176–188.
- Kirby BB, Takada N, Latimer AJ, Shin J, Carney TJ, Kelsh RN, et al. 2006. *In vivo* time-lapse imaging shows dynamic oligodendrocyte progenitor behavior during zebrafish development. *Nat Neurosci* 9(12):1506–1511, PMID: 17099706, <https://doi.org/10.1038/nn1803>.
- Koch M. 1999. The neurobiology of startle. *Prog Neurobiol* 59(2):107–128, PMID: 10463792, [https://doi.org/10.1016/S0301-0082\(98\)00098-7](https://doi.org/10.1016/S0301-0082(98)00098-7).
- Köhler S, Carmody L, Vasilevsky N, Jacobsen JOB, Danis D, Gouridine JP, et al. 2019. Expansion of the Human Phenotype Ontology (HPO) knowledge base and resources. *Nucleic Acids Res* 47(D1):D1018–D1027, PMID: 30476213, <https://doi.org/10.1093/nar/gky1105>.
- Kolodziejczyk K, Saab AS, Nave K-A, Attwell D. 2010. Why do oligodendrocyte lineage cells express glutamate receptors? *F1000 Biol Rep* 2:57, PMID: 21173873, <https://doi.org/10.3410/B2-57>.
- Konietschke F, Placzek M, Schaarschmidt F, Hothorn LA. 2015. nparcomp: an R software package for nonparametric multiple comparisons and simultaneous confidence intervals. *J Stat Softw* 64(9):1–17, <https://doi.org/10.18637/jss.v064.i09>.

- Kucenas S, Snell H, Appel B. 2008. *nkx2.2a* promotes specification and differentiation of a myelinating subset of oligodendrocyte lineage cells in zebrafish. *Neuron Glia Biol* 4(2):71–81, PMID: 19737431, <https://doi.org/10.1017/S1740925X0990123>.
- Lefebvre KA, Hendrix A, Halaska B, Duignan P, Shum S, Isoherranen N, et al. 2018. Domoic acid in California sea lion fetal fluids indicates continuous exposure to a neuroteratogen poses risks to mammals. *Harmful Algae* 79:53–57, PMID: 30420016, <https://doi.org/10.1016/j.hal.2018.06.003>.
- Lefebvre KA, Noren DP, Schultz IR, Bogard SM, Wilson J, Eberhart BTL. 2007. Uptake, tissue distribution and excretion of domoic acid after oral exposure in coho salmon (*Oncorhynchus kisutch*). *Aquat Toxicol* 81(3):266–274, PMID: 17250904, <https://doi.org/10.1016/j.aquatox.2006.12.009>.
- Lefebvre KA, Robertson A. 2010. Domoic acid and human exposure risks: a review. *Toxicol* 56(2):218–230, PMID: 19505488, <https://doi.org/10.1016/j.toxicol.2009.05.034>.
- Levin ED, Pang WG, Harrison J, Williams P, Petro A, Ramsdell JS. 2006. Persistent neurobehavioral effects of early postnatal domoic acid exposure in rats. *Neurotoxicol Teratol* 28(6):673–680, PMID: 17046199, <https://doi.org/10.1016/j.ntt.2006.08.005>.
- Levin ED, Pizarro K, Pang WG, Harrison J, Ramsdell JS. 2005. Persisting behavioral consequences of prenatal domoic acid exposure in rats. *Neurotoxicol Teratol* 27(5):719–725, PMID: 16054336, <https://doi.org/10.1016/j.ntt.2005.06.017>.
- Lyons DA, Talbot WS. 2015. Glial cell development and function in zebrafish. *Cold Spring Harb Perspect Biol* 7(2):a020586, <https://doi.org/10.1101/cshperspect.a020586>.
- Mariën K. 1996. Establishing tolerable dungeness crab (*Cancer magister*) and razor clam (*Siliqua patula*) domoic acid contaminant levels. *Environ Health Perspect* 104(11):1230–1236, PMID: 8959413, <https://doi.org/10.1289/ehp.104-1469507>.
- Marriott AL, Ryan CL, Doucette TA. 2012. Neonatal domoic acid treatment produces alterations to prepulse inhibition and latent inhibition in adult rats. *Pharmacol Biochem Behav* 103(2):338–344, PMID: 22981693, <https://doi.org/10.1016/j.pbb.2012.08.022>.
- Marsden KC, Granato M. 2015. In vivo Ca²⁺ imaging reveals that decreased dendritic excitability drives startle habituation. *Cell Rep* 13(9):1733–1740, PMID: 26655893, <https://doi.org/10.1016/j.celrep.2015.10.060>.
- März M, Schmidt R, Rastegar S, Strähle U. 2011. Regenerative response following stab injury in the adult zebrafish telencephalon. *Dev Dyn* 240(9):2221–2231, PMID: 22016188, <https://doi.org/10.1002/dvdy.22710>.
- Matute C, Domercq M, Sánchez-Gómez M-V. 2006. Glutamate-mediated glial injury: mechanisms and clinical importance. *Glia* 53(2):212–224, PMID: 16206168, <https://doi.org/10.1002/glia.20275>.
- Maucher JM, Ramsdell JS. 2005. Domoic acid transfer to milk: evaluation of a potential route of neonatal exposure. *Environ Health Perspect* 113(4):461–464, PMID: 15811837, <https://doi.org/10.1289/ehp.7649>.
- Maucher JM, Ramsdell JS. 2007. Maternal–fetal transfer of domoic acid in rats at two gestational time points. *Environ Health Perspect* 115(12):1743–1746, PMID: 18087593, <https://doi.org/10.1289/ehp.10446>.
- McDonald JW, Althomsons SP, Hyrc KL, Choi DW, Goldberg MP. 1998. Oligodendrocytes from forebrain are highly vulnerable to AMPA/kainate receptor-mediated excitotoxicity. *Nat Med* 14:291–297, <https://doi.org/10.1038/nm0398-291>.
- Mokalled MH, Patra C, Dickson AL, Endo T, Stainier DFR, Poss KD. 2016. Injury-induced *ctgfa* directs glial bridging and spinal cord regeneration in zebrafish. *Science* 354(6312):630–634, PMID: 27811277, <https://doi.org/10.1126/science.aaf2679>.
- Munzel U, Hothorn LA. 2001. A unified approach to simultaneous rank test procedures in the unbalanced one-way layout. *Biom J* 43(5):553–569, [https://doi.org/10.1002/1521-4036\(200109\)43:5<553::AID-BIMJ553>3.0.CO;2-N](https://doi.org/10.1002/1521-4036(200109)43:5<553::AID-BIMJ553>3.0.CO;2-N).
- Niemann A, Berger P, Suter U. 2006. Pathomechanisms of mutant proteins in Charcot-Marie-Tooth disease. *Neuromolecular Med* 8(1–2):217–241, PMID: 16775378, <https://doi.org/10.1385/nmm.8:1-2.217>.
- O'Malley DM, Kao Y-H, Fetcho JR. 1996. Imaging the functional organization of zebrafish hindbrain segments during escape behaviors. *Neuron* 17(6):1145–1155, PMID: 8982162, [https://doi.org/10.1016/S0896-6273\(00\)80246-9](https://doi.org/10.1016/S0896-6273(00)80246-9).
- Orger MB, de Polavieja GG. 2017. Zebrafish behavior: Opportunities and Challenges. *Annu Rev Neurosci* 40:125–147, PMID: 28375767, <https://doi.org/10.1146/annurev-neuro-071714-033857>.
- Pajević S, Bassler PJ, Fields RD. 2014. Role of myelin plasticity in oscillations and synchrony of neuronal activity. *Neuroscience* 276:135–147, PMID: 24291730, <https://doi.org/10.1016/j.neuroscience.2013.11.007>.
- Panlilio JM. 2019. Ph.D. Thesis: Impacts of developmental exposures to the harmful algal bloom toxin domoic acid on neural development and behavior, MIT/WHOI Joint Graduate Program in Oceanography and Oceanographic Engineering. <https://hdl.handle.net/1912/24081> [accessed 7 October 2020].
- Panula P, Chen YC, Priyadarshini M, Kudo H, Semenova S, Sundvik M, Sallinen V. 2010. The comparative neuroanatomy and neurochemistry of zebrafish CNS systems of relevance to human neuropsychiatric diseases. *Neurobiol Dis* 40(1):46–57, PMID: 20472064, <https://doi.org/10.1016/j.nbd.2010.05.010>.
- Patneau DK, Wright PW, Winters C, Mayer ML, Gallo V. 1994. Glial cells of the oligodendrocyte lineage express both kainate- and AMPA-preferring subtypes of glutamate receptor. *Neuron* 12(2):357–371, PMID: 7509160, [https://doi.org/10.1016/0896-6273\(94\)90277-1](https://doi.org/10.1016/0896-6273(94)90277-1).
- Pekny M, Nilsson M. 2005. Astrocyte activation and reactive gliosis. *Glia* 50(4):427–434, PMID: 15846805, <https://doi.org/10.1002/glia.20207>.
- Perl TM, Bédard L, Kosatsky T, Hockin JC, Todd EC, McNutt LA, et al. 1990a. Amnesic shellfish poisoning: a new clinical syndrome due to domoic acid. *Can Dis Wkly Rep* 16(suppl 1E):7–8, PMID: 2101742.
- Perl TM, Bédard L, Kosatsky T, Hockin JC, Todd EC, Remis RS. 1990b. An outbreak of toxic encephalopathy caused by eating mussels contaminated with domoic acid. *N Engl J Med* 322(25):1775–1780, PMID: 1971709, <https://doi.org/10.1056/NEJM199006213222504>.
- Perry MA, Ryan CL, Tasker RA. 2009. Effects of low dose neonatal domoic acid administration on behavioural and physiological response to mild stress in adult rats. *Physiol Behav* 98(1–2):53–59, PMID: 19375434, <https://doi.org/10.1016/j.physbeh.2009.04.009>.
- Petroff R, Richards T, Crouthamel B, McKain N, Stanley C, Grant KS, et al. 2019. Chronic, low-level oral exposure to marine toxin, domoic acid, alters whole brain morphometry in nonhuman primates. *Neurotoxicology* 72:114–124, PMID: 30826346, <https://doi.org/10.1016/j.neuro.2019.02.016>.
- Pogoda H-M, Sternheim N, Lyons DA, Diamond B, Hawkins TA, Woods IG, et al. 2006. A genetic screen identifies genes essential for development of myelinated axons in zebrafish. *Dev Biol* 298(1):118–131, PMID: 16875686, <https://doi.org/10.1016/j.ydbio.2006.06.021>.
- Preston E, Hynne I. 1991. Transfer constants for blood-brain barrier permeation of the neuroexcitatory shellfish toxin, domoic acid. *Can J Neurol Sci* 18(1):39–44, PMID: 2036614, <https://doi.org/10.1017/S0317167100031279>.
- Pulido OM. 2008. Domoic acid toxicology pathology: a review. *Mar Drugs* 6(2):180–219, PMID: 18728725, <https://doi.org/10.3390/md6020180>.
- Reimand J, Arak T, Adler P, Kolberg L, Reisberg S, Peterson H, et al. 2016. g:Profiler—a web server for functional interpretation of gene lists (2016 update). *Nucleic Acids Res* 44(W1):W83–W89, PMID: 27098042, <https://doi.org/10.1093/nar/gkw199>.
- Rice D, Barone S Jr. 2000. Critical periods of vulnerability for the developing nervous system: evidence from humans and animal models. *Environ Health Perspect* 108(suppl 3):511–533, PMID: 10852851, <https://doi.org/10.1289/ehp.00108s3511>.
- Robinson MD, McCarthy DJ, Smyth GK. 2010. edgeR: a Bioconductor package for differential expression analysis of digital gene expression data. *Bioinformatics* 26(1):139–140, PMID: 19910308, <https://doi.org/10.1093/bioinformatics/btp616>.
- Rosario-Martinez HD, Fox J. 2015. Post-hoc interaction analysis. <https://cran.r-project.org/web/packages/phia/phia.pdf> [accessed 7 October 2020].
- Rust L, Gulland F, Frame E, Lefebvre K. 2014. Domoic acid in milk of free living California marine mammals indicates lactational exposure occurs. *Mar Mamm Sci* 30(3):1272–1278, <https://doi.org/10.1111/mms.12117>.
- Sánchez-Gómez MV, Matute C. 1999. AMPA and kainate receptors each mediate excitotoxicity in oligodendroglial cultures. *Neurobiol Dis* 6(6):475–485, <https://doi.org/10.1006/nbdi.1999.0264>.
- Schneider H, Klee EW, Clark KJ, Petzold AM, Mock VL, Abarr JM, et al. 2012. Zebrafish and drug development: a behavioral assay system for probing nicotine function in larval zebrafish. In: *Zebrafish Protocols for Neurobehavioral Research*. Kaluuff A, Stewart A, eds. Totowa, NJ: Humana Press, 53–70.
- Scholin CA, Gulland F, Doucette GJ, Benson S, Busman M, Chavez FP, et al. 2000. Mortality of sea lions along the central California coast linked to a toxic diatom bloom. *Nature* 403(6765):80–84, PMID: 10638756, <https://doi.org/10.1038/47481>.
- Shiotani M, Cole TB, Hong S, Park JY, Griffith WC, Burbacher TM, et al. 2017. Neurobehavioral assessment of mice following repeated oral exposures to domoic acid during prenatal development. *Neurotoxicol Teratol* 64:8–19, PMID: 28916171, <https://doi.org/10.1016/j.ntt.2017.09.002>.
- Shum S, Jing J, Petroff R, Crouthamel B, Grant KS, Burbacher TM, et al. 2020. Maternal-fetal disposition of domoic acid following repeated oral dosing during pregnancy in nonhuman primate. *Toxicol Appl Pharmacol* 398:115027, PMID: 32360744, <https://doi.org/10.1016/j.taap.2020.115027>.
- Skaggs K, Goldman D, Parent JM. 2014. Excitotoxic brain injury in adult zebrafish stimulates neurogenesis and long-distance neuronal integration. *Glia* 62(12):2061–2079, PMID: 25043622, <https://doi.org/10.1002/glia.22726>.
- Sumbre G, de Polavieja GG. 2014. The world according to zebrafish: how neural circuits generate behavior. *Front Neural Circuits* 8:91, PMID: 25126059, <https://doi.org/10.3389/fncir.2014.00091>.
- Suzuki CAM, Hierlihy SL. 1993. Renal clearance of domoic acid in the rat. *Food Chem Toxicol* 31(10):701–706, PMID: 8225127, [https://doi.org/10.1016/0278-6915\(93\)90140-T](https://doi.org/10.1016/0278-6915(93)90140-T).
- Tanaka S, Mito T, Takashima S. 1995. Progress of myelination in the human fetal spinal nerve roots, spinal cord and brainstem with myelin basic protein immunohistochemistry. *Early Hum Dev* 41(1):49–59, PMID: 7540130, [https://doi.org/10.1016/0378-3782\(94\)01608-R](https://doi.org/10.1016/0378-3782(94)01608-R).

- Tanemura K, Igarashi K, Matsugami T-R, Aisaki K, Kitajima S, Kanno J. 2009. Intrauterine environment–genome interaction and children’s development (2): brain structure impairment and behavioral disturbance induced in male mice offspring by a single intraperitoneal administration of domoic acid (DA) to their dams. *J Toxicol Sci* 34(suppl 2):SP279–SP286, PMID: 19571481, <https://doi.org/10.2131/jts.34.SP279>.
- Tasker RAR, Perry MA, Doucette TA, Ryan CL. 2005. NMDA receptor involvement in the effects of low dose domoic acid in neonatal rats. *Amino Acids* 28(2):193–196, PMID: 15714252, <https://doi.org/10.1007/s00726-005-0167-z>.
- Teitelbaum JS, Zatorre RJ, Carpenter S, Gendron D, Evans AC, Gjedde A, et al. 1990. Neurologic sequelae of domoic acid intoxication due to the ingestion of contaminated mussels. *N Engl J Med* 322(25):1781–1787, PMID: 1971710, <https://doi.org/10.1056/NEJM199006213222505>.
- Tiedeken JA, Ramsdell JS. 2007. Embryonic exposure to domoic acid increases the susceptibility of zebrafish larvae to the chemical convulsant pentyleneetetrazole. *Environ Health Perspect* 115(11):1547–1552, PMID: 18007982, <https://doi.org/10.1289/ehp.10344>.
- Tiedeken JA, Ramsdell JS, Ramsdell AF. 2005. Developmental toxicity of domoic acid in zebrafish (*Danio rerio*). *Neurotoxicol Teratol* 27(5):711–717, PMID: 16061356, <https://doi.org/10.1016/j.ntt.2005.06.013>.
- Tropepe V, Sive HL. 2003. Can zebrafish be used as a model to study the neurodevelopmental causes of autism? *Genes Brain Behav* 2(5):268–281, PMID: 14606692, <https://doi.org/10.1034/j.1601-183X.2003.00038.x>.
- Tryphonas L, Truelove J, Nera E, Iverson F. 1990. Acute neurotoxicity of domoic acid in the rat. *Toxicol Pathol* 18(1 pt 1):1–9, PMID: 2362984, <https://doi.org/10.1177/019262339001800101>.
- Verity AN, Campagnoni AT. 1988. Regional expression of myelin protein genes in the developing mouse brain: in situ hybridization studies. *J Neurosci Res* 21(2–4):238–248, PMID: 2464076, <https://doi.org/10.1002/jnr.490210216>.
- Wang GJ, Schmued LC, Andrews AM, Scallet AC, Slikker W Jr, Binienda Z. 2000. Systemic administration of domoic acid-induced spinal cord lesions in neonatal rats. *J Spinal Cord Med* 23(1):31–39, PMID: 10752872, <https://doi.org/10.1080/10790268.2000.11753506>.
- Venables WN, Ripley BD. 2002. *Modern Applied Statistics with S*. 4th ed. New York: Springer.
- Wekell JC, Gauglitz EJ Jr, Bamett HJ, Hatfield CL, Simons D, Ayres D. 1994. Occurrence of domoic acid in Washington State razor clams (*Siliqua patula*) during 1991–1993. *Nat Toxins* 2(4):197–205, PMID: 7952944, <https://doi.org/10.1002/nt.2620020408>.
- Wekell JC, Hurst J, Lefebvre KA. 2004. The origin of the regulatory limits for PSP and ASP toxins in shellfish. *J Shellfish Res* 23(3):927–930.
- Wen H-L, Lin Y-T, Ting C-H, Lin-Chao S, Li H, Hsieh-Li HM. 2010. Stathmin, a microtubule-destabilizing protein, is dysregulated in spinal muscular atrophy. *Hum Mol Genet* 19(9):1766–1778, PMID: 20176735, <https://doi.org/10.1093/hmg/ddq058>.
- Wen H-L, Ting C-H, Liu H-C, Li H, Lin-Chao S. 2013. Decreased stathmin expression ameliorates neuromuscular defects but fails to prolong survival in a mouse model of spinal muscular atrophy. *Neurobiol Dis* 52:94–103, PMID: 23268200, <https://doi.org/10.1016/j.nbd.2012.11.015>.
- Wobbrock JO, Findlater L, Gergle D, Higgins JJ. 2011. The aligned rank transform for nonparametric factorial analyses using only ANOVA procedures. In: *Proceedings of the SIGCHI Conference on Human Factors in Computing Systems*. May 2011. New York, NY: Association for Computing Machinery, 143–146.
- Wolman MA, Jain RA, Liss L, Granato M. 2011. Chemical modulation of memory formation in larval zebrafish. *Proc Natl Acad Sci USA* 108(37):15468–15473, PMID: 21876167, <https://doi.org/10.1073/pnas.1107156108>.
- Xi D, Peng YG, Ramsdell JS. 1997. Domoic acid is a potent neurotoxin to neonatal rats. *Nat Toxins* 5(2):74–79, PMID: 9131593, [https://doi.org/10.1002/\(SICI\)199705:2<74::AID-NT4>3.0.CO;2-I](https://doi.org/10.1002/(SICI)199705:2<74::AID-NT4>3.0.CO;2-I).
- Xie J, Farage E, Sugimoto M, Anand-Apte B. 2010. A novel transgenic zebrafish model for blood-brain and blood-retinal barrier development. *BMC Dev Biol* 10:76, PMID: 20653957, <https://doi.org/10.1186/1471-213X-10-76>.
- Yeomans JS, Frankland PW. 1995. The acoustic startle reflex: neurons and connections. *Brain Res Brain Res Rev* 21(3):301–314, PMID: 8806018, [https://doi.org/10.1016/0165-0173\(96\)00004-5](https://doi.org/10.1016/0165-0173(96)00004-5).
- Yuan A, Rao MV, Veeranna, Nixon RA. 2012. Neurofilaments at a glance. *J Cell Sci* 125(pt 14):3257–3263, PMID: 22956720, <https://doi.org/10.1242/jcs.104729>.
- Zuloaga DG, Lahvis GP, Mills B, Pearce HL, Turner J, Raber J. 2016. Fetal domoic acid exposure affects lateral amygdala neurons, diminishes social investigation and alters sensory-motor gating. *Neurotoxicology* 53:132–140, PMID: 26797589, <https://doi.org/10.1016/j.neuro.2016.01.007>.